Appendix 6

Mineralogy and geochemistry of redox front I (RFI).

Contents

		page
1.	Introduction	413
2.	Field observations and sampling	413
3.	Macroscopic descriptions and sample preparation	415
3.1.	Macroscopic descriptions	415
3.2.	Sample preparation	419
4.	Mineralogy and petrography	419
4.1.	Non-mineralised rocks	419
4.2.	Mineralised rocks	422
4.3.	X-ray diffraction (XRD) studies	426
5.	Rock physical parameters	428
6.	Geochemistry	429
6.1.	Sample preparation and analysis	429
6.2.	Geochemistry of sample set I (large-sized samples)	433
6.3.	Geochemistry of sample set II (main XRF samples)	434
6.3.1.	RFI phonolites: magmatic composition and hydrothermally altered potassic rock	435
6.3.2.	RFI oxidised and reduced phonolites	444
6.3.3.	RFI redox front processes	446
7.	Summary	460
8.	References	462
	APPENDICES:	
	Appendix 6:1: PLATES 6:1-1 – 6:1-9	465
	Appendix 6:2: Rock chemical data for RFI	477

Appendix 6
Mineralogy and geochemistry of redox front I (RFI).

H.D. SCHORSCHER

Universidade de São Paulo, Instituto de Geociências-DMP, C.P. 20 899,
014 98 São Paulo (Brazil).

1. Introduction

Redox front I (RFI) was sampled from the Osamu Utsumi uranium mine (open pit, coordinates 8.2BJ.61). Two sample sets were prepared for distribution; one set for measurements of natural Pu and Tc, and the other for radiochemistry and global geochemistry.

Mineralogical, petrographic and geochemical studies were carried out at the University of Bern using routine XRF major and trace element analysis, together with the determination of rock physical parameters.

2. Field observations and sampling

RFI constitutes a complete profile across oxidised phonolite, the redox front sensu strictu and the reduced phonolite. On the reduced side, about 10 cm away from the redox front, a zone of secondary nodular U-mineralisation begins. This zone is about 30 cm wide and grades away from the front, accompanied by the disappearance of U-nodules into the reduced country phonolite.

The phonolite is an extremely fine-grained, almost aphanitic rock containing only subordinate coarser components (phenocrysts and microxenoliths). The oxidised phonolite is a light yellow/brown colour and the reduced phonolite is light to medium grey in colour.

The total width of the exposed profile was about 3 metres. Sampling was conducted systematically through the oxidised portion, the redox front, and included about 50 cm of the adjacent reduced phonolite, which contained the zone of secondary U-mineralisation. Following this, two sampling intervals of about 35 and 100 cm were selected within the reduced country phonolite further away from the redox front. Figure 6-1 gives a schematic view of the original outcrop situation and of the approximate spacial

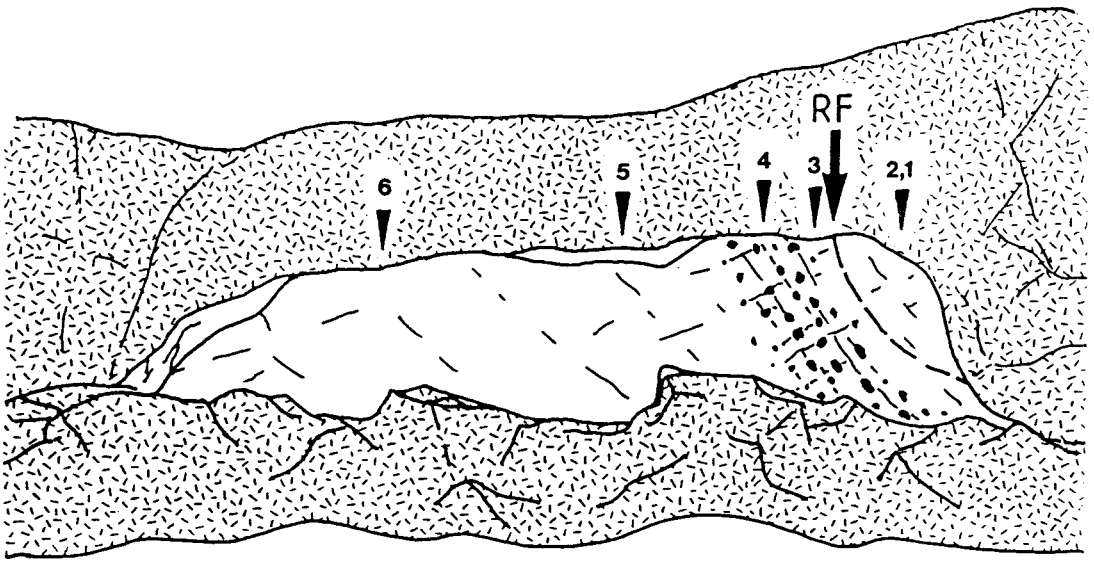

Figure 6-1. Schematic view of the original outcrop situation at the RFI sampling site (scale 3 m long). Indicated are the approximate positions of the redox front (RF) and of the sampling locations RFI 1 to 6. Oxidised rocks occur on the right-hand side of the redox front and reduced rocks on the left. The zone of maximum U-mineralisation is indicated by black dots representing pitchblende nodules (Osamu Utsumi uranium mine, coordinates: 8.2 BJ.61, view towards the E).

and structural relationships of the collected samples. The individual samples were medium-sized, weighing between 8 and 15 kg each.

3. Macroscopic descriptions and sample preparation

3.1. Macroscopic descriptions

Detailed sample descriptions have been carried out and the various textural features illustrated in Plates 6:1-1 to 6:1-6 (Appendix 6:1); summarised sample descriptions and radioactivity measurements are contained in Table 6-I. Briefly, the RFI rocks suffered hydrothermal and supergenic alteration, following the early magmatic genetic stage; the supergene alteration occurred under reducing conditions or reducing conditions followed by oxidising conditions. The reduced RFI rocks furthest from the redox front (Fig. 6-1, samples RFI-5 and -6; Plates 6:1-5 and 6:1-6) have best preserved the primary magmatic and subsequent hydrothermal properties.

The main host rock is a very fine-grained, almost aphanitic phonolite of light to medium grey colour. It is normally only weakly porphyritic and microxenolithic (Plate 6:1-5), although in sample RFI-6 (Plate 6:1-6) there occurs one larger nepheline syenite xenolith. Phenocrysts consist of pseudoleucite, alkali feldspar and (pseudomorphosed) nepheline; microxenoliths of nepheline syenite and phonolite fragments also occur.

Hydrothermal effects include mainly the porous leaching of pseudoleucite phenocrysts, (micro-)xenoliths of nepheline syenites (Plate 6:1-6) and coarser-grained phonolites, and the disseminated pyritisation of the rocks and fracture planes.

The supergenic processes led to the development of the redox fronts which are locally associated with secondary U-mineralisations occurring on the reduced sides, and generally associated with the precipitation of hydrous ferric oxides (HFO) on the oxidised sides of the fronts.

The RFI redox front is easily recognisable due to the sharply developed colour contrast between the HFO-bearing oxidised and pyrite-bearing reduced rocks (Plates 6:1-1 and 6:1-2). The secondary supergenic U-mineralisation concentrates in the reduced rocks (Plates 6:1-3 and 6:1-4), forming a zone of variable width (20 – 30 cm) extending almost parallel to the redox front.

The mineralised zone, however, starts only some 5 to 10 cm ahead of the HFO precipitation front located inside the pyrite domain (Plate 6:1-3). The U-mineralisation consists of black coloured aggregates of cryptocrystalline oxides occurring either as

TABLE 6-I
Summarised macroscopic petrography of RFI samples (see Fig. 6-1 for sample location).

Current no.	Sample code	Sample description	Radioactivity cps above bg	Refer to PLATES in Appendix 6:1
1	RFI-1	Oxidised, light-yellow/brown in colour, very fine-grained microporphyritic and microxenolithic phonolite. The sample extends from about 30 cm in the host rock to the redox front. It shows a homogeneous and oscillatory zoned hydrous ferric oxide (mainly limonite) distribution, and contains bleached, whitish coloured residual nodules resulting from pitchblende dissolution.	30	
2	RFI-2	Rock composed mainly of oxidised and minor reduced phonolite, including the redox front. The sample extends from about 25 cm before the redox front to about 10 cm into the reduced phonolite, and represents the physical continuation of sample RFI-1. Only the reduced phonolite differs, being light-grey in colour, characterised by finely disseminated pyrite and is free of HFO minerals.	30 (10 cm before RF); 50 (Zone rich in HFO close to RF); 50 (Reduced side close to RF);	6:1-1; 6:1-2
3	RFI-3	Rock composed mainly of reduced phonolite, minor oxidised phonolite, including the redox front. The reduced phonolite is characterised by a 10 cm zone immediately adjacent to the redox front which is free of nodular U-mineralisation. This zone soon gives way to the appearance of pitchblende nodules and eventually to the zone of maximum mineralisation.	50 (Zone of 10 cm near RF); 95 (Transition to U-mineralised zone);	6:1-3

TABLE 6-I (contd.).

Current no.	Sample code	Sample description	Radioactivity cps above bg	Refer to PLATES in Appendix 6:1
4	RFI-4	Reduced phonolite selected from zone of maximum secondary (redox front-related) U-mineralisation. Pitchblende nodules of various dimensions, forms and internal textures are always controlled by fracture systems. The pitchblende nodules are commonly richer in pyrite than the enclosing reduced phonolite. The reduced rock portions consists of a very fine-grained microporphyritic and -xenolithic phonolite similar to that described above. The sample represents the profile portion which grades away from the redox front, accompanied by the disappearance of pitchblende nodules, into the normal (macroscopically non-mineralised) reduced country phonolite.	120 (Zone of max. U-mineralisation);	6:1-4
5	RFI-5	Reduced country phonolite (macroscopically non-mineralised), collected about 35 cm from sample RFI-4 within a homogeneous sequence of rock composition.	15 (Reduced country phonolite);	6:1-5
6	RFI-6	Reduced country phonolite (macroscopically non-mineralised) containing a major xenolith of reduced nepheline syenite. The sample was collected about 1 m from sample RFI-5 in a sequence of macroscopically homogeneous phonolites.	15 (Reduced country phonolite);	6:1-6

nodular concretions of rounded, elliptical or, more rarely, irregular forms of pitchblende (of submillimetric to centimetric dimensions and sometimes showing zoning structures; Plates 6:1-3 and 6:1-4), or as very fine, normally submillimetric coatings on fracture surfaces (Plate 6:1-3). The secondary U-mineralisations are always enriched in pyrite compared to the host (reduced) rocks.

Genetically and structurally it is significant that the formation and preferential development of both types of secondary U-mineralisation are controlled by fractures/fracture systems (Plates 6:1-3 and 6:1-4).

Within the 5 – 10 cm zone of reduced rocks closest to the HFO front, the progressive and normally complete dissolution of the U-mineralisation still occurs under the continuing presence of pyrite. In the oxidised rocks, secondary U-oxide mineralisation is absent, except for rare cases of preserved relicts that survived (in association with pyrite) in reducing micro-environments entirely included by the oxidised rocks. The total dissolution of secondary U-mineralisation results in bleached, white-coloured, pyrite-free rock portions that precisely demarcate the original extent of the mineralisation (Plates 6:1-1 and 6:1-2). It is important to note that the precipitation of HFO minerals (from the pyrite oxidation) was not coeval with U-oxide dissolution. It seems that the higher pyrite contents of the U-nodules (this report; Appendix 1, Fig. 1-13) and their dissolution, leading to a low pH acidic environment, favoured the fairly complete removal of the originally indigenous nodule (Blanchard, 1968).

In the oxidised rocks, similar magmatic and hydrothermal features were developed as described for the reduced phonolites. However, these were modified and less well preserved, due particularly to the oxidic-supergenic overprinting. The latter resulted in higher rock porosities and permeabilities due to general pyrite dissolution that was only partially compensated for by the overall HFO precipitation. These tend to be distributed homogeneously to inhomogeneously throughout the rocks. In the RFI oxidised rocks the HFO distribution is irregular, with some rock portions showing homogeneously dispersed HFO and others showing millimetrically fine rhythmic zoning (Plates 6:1-1 and 6:1-2). The origin of the rhythmic zoning is not known but may be related to seasonal oscillations of the water table and/or to climatic changes. Former secondary U-oxide mineralisations can be recognised by matching areas of bleached rock (Plates 6:1-1 and 6:1-2). However, the distribution of radioactivity, as shown by scintillometry, is irregular in the oxidised rocks. Higher radioactivity occurs in the rock portions richer in HFO, indicating the fixation of (mainly) U to the Fe-oxyhydroxides, probably by co-precipitation.

3.2. Sample preparation

Detailed macroscopic studies determined the samples selected for the mineralogical and geochemical studies. A total of 10 thin sections, 5 polished sections and 7 polished thin sections were prepared for light-optical, petrographic and ore microscopy. Selective powder samples for complementary mineralogical XRD studies were extracted from the bulk rocks, together with other features of interest such as secondary nodular U-mineralisations and their dissolution-bleached equivalents.

For geochemical studies two representative sample sets were selected; large-sized samples (decimetric) of the major zones distinguishing the RFI front, and smaller, more densely sampled sets (centimetric) to better define the small-scale variations. Finally, a set of samples for determining rock physical parameters was selected. Table 6-II presents sample details and the nature of the performed studies.

4. Mineralogy and petrography

4.1. Non-mineralised rocks

The main phonolites of the RFI profile are quite homogeneous, extremely fine-grained (almost aphanitic) and contain only subordinate amounts of microphenocrysts and microxenoliths. The mean grain-size of the phonolite was estimated from the major constituents, i.e. sanidine laths and prisms, and ranges from 0.02 – 0.04 mm. These have survived hydrothermal and supergene processes without any major textural alteration. The other major silicate minerals comprise sericite/illite (white micas) and kaolinite and are products of hydrothermal replacement. Semi-translucent minerals include Ti-oxides (rutile) in the reduced rocks and HFO minerals (mainly limonite) and Ti-oxides in the oxidised rocks. Opaque minerals consist mainly of cube-shaped pyrite microcrystals that occur exclusively in the reduced rocks; the pyrites are free of inclusions and are freshly preserved. Due to the extremely fine grain-size of the RFI rocks, volumetric estimates are problematic. However, the best possible approximations are given in Table 6-III, which considered the original magmatic, hydrothermal and supergene minerals.

Textural evidence shows that the main RFI phonolites are of very shallow subvolcanic to extrusive origin. The low zircon contents indicate that these phonolites were not affected by higher grade hydrothermal U-Zr-REE mineralisation.

TABLE 6-II
Sample details and studies performed.

Number of original sample	Sample splits prepared according to petrographic zones: No.	Petrography	Geochemistry: analytical sets and nos.: I-various methods	II-Univ. Bern: XRF	II-Univ. Bern: Cd-AAS	Other studies: Rock physical parameters	Other studies: X-ray diffraction	Other studies: Optical mineralogy, petrography	Refer to PLATES in Appendix 6:1
RFI-1	1A	Oxidised rock: 25-15 cm from redox front (2 identical splits)	03 –	– RFI-1A	03 2	– RFI-1A	I-A I.3	+ +	– –
	1B	Oxidised rock: 15-5 cm from redox front with bleached nodules	–	RFI-1B	1, 3[1)]	RFI-1B	I-B I.1 I.2	+	–
	1C	Oxidised rock: 5 cm adjacent to redox front	–	RFI-1C	–	RFI-1C	–	+	–
	1D	Reduced rock: ≤ 3 cm adjacent to redox front	–	–	–	–	–	+	–
RFI-2	2A	Oxidised rock: 25-10 cm from redox front, with bleached nodules	–	–	1, 3[1)]	–	–	+	–
	2B	Oxidised rock: 10 cm adjacent to redox front	04	–	04 -	–	–	+	6:1-1, 6:1-2
	2C	Reduced rock: 0-~10 cm adjacent to redox front, non-mineralised	–	–	4	–	II I.4	+	6:1-1, 6:1-2
RFI-3	3A	Oxidised rock: ~3 cm adjacent to redox front	–	–	–	–	–	+	6:1-3
	3B	Reduced rock: non-mineralised zone of ~10 cm adjacent to redox front (2 identical splits)	05 –	– RFI-3	05 5	– RFI-3	I.5 –	+ +	6:1-3 6:1-3

TABLE 6-II (contd.).

Number of original sample	Sample splits prepared according to petrographic zones: No.	Petrography	Geochemistry: analytical sets and nos.: I-various methods	II-Univ. Bern: XRF	II-Univ. Bern: Cd-AAS	Other studies: Rock physical parameters	Other studies: X-ray diffraction	Other studies: Optical mineralogy petrography	Refer to PLATES in Appendix 6:1
RFI-3 (contd.)	3C	Reduced rock: 0-≤ 5 cm of mineralised zone with abundant U-macronodules	–	–	–	–	III	+	6:1-3
RFI-4	4A-1	Reduced rock: mineralised zone with U-micronodules	–	RFI-4A-1	–	–	–	+	–
	4A-2	Reduced rock: mineralised zone without U-nodules	–	RFI-4A-2	–	–	–	+	–
	4B	Reduced rock: max. mineralised zone with abundant U-macronodules (2 identical splits)	06 –	– RFI-4B	06 6, 7	– RFI-4B	– I.6 I.7	+ +	6:1-4 6:1-4
	4C	Reduced rock: transition to non-mineralised phonolite	–	–	–	–	–	+	–
RFI-5	5A	Reduced phonolite, non-mineralised	–	RFI-5A	–	RFI-5A	–	+	6:1-5
	5B	Reduced phonolite, weakly mineralised (2 identical splits)	07 –	– RFI-5B	07 –	– RFI-5B	– –	+ +	– –
RFI-6	6A	Reduced phonolite, non-mineralised	–	–	–	–	–	+	6:1-6
	6B	Reduced nepheline syenite xenolith	–	RFI-6B	–	RFI-6B	–	+	6:1-6

[1]Mixed samples of RFI-1B and RFI-2A.

4.2. Mineralised rocks

The phonolites of the mineralised zone (Plates 6:1-3 and 6:1-4) are identical in composition with the non-mineralised rocks (Table 6-III), except for the pitchblende nodules and their bleached equivalents in the case of oxidised, formerly mineralised phonolites (Plates 6:1-1 and 6:1-2). The pitchblende nodules consist of cryptocrystalline U-oxides precipitated along grain boundaries and in (micro-)pores and interstices of the rock. These precipitations form intergranular films and aggregates, causing partial to total pore fillings. The U-oxides are accompanied by the precipitation of a second generation of pyrites, but only in the inside of the nodules. Both processes effectively diminish the microporosity of the reduced rocks. The second generation pyrites are frequently coarser-grained than the earlier varieties and may even include them. Both pyrite generations are freshly preserved and show no differences in colour or reflectivity. The substitution of rock-forming minerals by pitchblende and/or second generation pyrites could not be verified microscopically. Doubtless there exists a growth process of the nodules. This can be described, based on mineralogical-textural grounds, as originating from some point source and subsequently being followed by centrifugal spreading and growth controlled by fracture planes and grain boundaries, and the infiltration and the filling of micropores with U-oxides and pyrites. Regular (concentric) and irregular zoned U-nodules are products of variable densities/concentrations of U-oxide precipitation (Plates 6:1-3 and 6:1-4). The reasons for the variable patterns of the U-oxide precipitation within isotropic igneous rocks are unknown and difficult to explain by purely inorganic processes.

In general, the pitchblende nodules can be considered to consist of cryptocrystalline U-oxides (see item 4.3, XRD studies), with crystallites dominating below the limit of microscopic resolution (magnification of about 1200 x). Aggregated masses of U-oxides are optically isotropic. The U-oxides are precipitated together with a second pyrite generation mainly available in natural open spaces (grain boundaries, rock pores, interstices) of the reduced rocks without any microscopically recognisable substitution of the rock-forming minerals. The sizes of the nodules range from microscopic (and even submicroscopic) dimensions, as a lower limit, to a maximum of a few centimetres. The nodular forms suggest either inorganic growth processes, e.g. ovoidal concretions or biogenic processes. The microtextures and mineral parageneses are interpreted as favouring the biogenic hypothesis. The nodules of the active redox fronts can be termed first generation nodules and are distinct in nature and origin from the massive secondary U-nodules described elsewhere. (Appendix 1).

During the advancement of the redox front, the pitchblende nodules of the mineralised rocks suffered dissolution still under reducing conditions, due to the continued stability of pyrite. This resulted in pitchblende-free zones directly adjacent to the redox fronts on the reduced side. The widths of these zones can vary from millimetres (or even submillimetres) to centimetres, as in the case of RFI. For comparison, an example of millimetre dimensions from another redox front is shown in Plate 6:1-7. These zones are also pyrite-bearing but normally distinctly white-coloured (due to the dissolution of black U-oxides) when compared to the adjacent mineralised (grey) and oxidised (yellowish-brown) rocks. Their compositions proved to be similar to those of the adjacent reduced rocks free of U-oxides, and they should not be confused with the clay mineral (e.g. kaolinite)-enriched zones. Plates 6:1-8 and 6:1-9 show pitchblende dissolution using detailed cathodoluminescence images.

Further advancement of the redox front finally leads to the complete oxidation and transformation of the formerly U-mineralised reduced rocks into oxidised varieties. Macroscopically, oxidation refers only to the precipitation of HFO minerals (mainly limonite) that give the oxidised rocks their typical yellowish-brown colouration (Plates 6:1-1, 6:1-2, 6:1-3 and 6:1-7). This oxidation process is already seen in the U-oxide-free rocks as a function of the availability of low pH solutions resulting from the oxidation of pyrite, which forms a variety of ferrous and ferric sulphates. In the presence of low sulphate concentrations all the oxidised Fe-pyrite is reprecipitated in situ as indigenous limonite, ideally without any pseudomorphism of the former pyrite microcrystals. At higher sulphate concentrations, mobilisation, oxidation and limited transport takes place, and reprecipitation as limonite occurs only after adequate dilution and hydrolysis. Limonite can be precipitated as new forms, independently of the former pyrite distribution, as homogeneous or inhomogeneous pigmentations. This generally affected the oxidised rocks, explaining their higher porosity resulting from pyrite dissolution, which was only incompletely compensated for by the reprecipitation of the HFO minerals (limonite). At highest original pyrite contents which have consequently resulted in the highest sulphate concentrations, all of the former Fe-pyrite is removed. Reprecipitation takes place elsewhere after sufficient transport has occurred to permit adequate dilution and hydrolysis. This is the case with the bleached nodules remaining from the final dissolution of the former pitchblende nodules (Plates 6:1-1 and 6:1-2), which contained a very high content of original pyrite. The bleached nodules achieve the highest porosity through these processes since pyrite dissolution is not compensated for by HFO mineral precipitation. Microscopically, the bleached nodules contain all the rock-forming minerals comprising the enclosing oxidised rocks, and are characterised by

TABLE 6-III

Modal compositions of RFI non-mineralised reduced and oxidised phonolites (numbers in brackets refer to totally replaced minerals).

Minerals	Vol.% Mean grain-size in mm Origin	Observations
Alkali feldspar phenocrysts	1 – 2 0.1 >5 magmatic	Former microperthitic orthoclases showing alkali exchange and indicating structural readjustment. Fluid inclusions and weak kaolinisation are also present. Pyrite and HFO mineral inclusions occur in both the reduced and oxidised rocks.
Pseudoleucite phenocrysts	tr. – 1 0.5 – >20 magmatic	Pseudomorphs composed of alkali feldspars, sericite/illite, kaolinite, pyrite and containing HFO minerals.
Nepheline phenocrysts	(tr. – 1) (0.1 – 3) magmatic	Replaced kaolinite, sericite/illite, pyrite and containing HFO minerals.
Aegirine-augite phenocrysts	(0 – tr.) (0.1 – 2) magmatic	Replaced by cryptocrystalline aggregates of TiO_2 minerals, kaolinite, unidentified clay minerals (? smectites), pyrite and containing HFO minerals.
Nepheline of the groundmass	(~10) (~0.02) magmatic	Replaced by kaolinite, sericite/illite, pyrite and containing HFO minerals.
Sanidine laths and prisms of the groundmass	55 – 65 0.02 – 0.04 magmatic	The main magmatic minerals show evidence of alkali exchange and structural readjustment. Some kaolinisation also occurs.
Aegirine-augite of the groundmass	(1 – 3) (0.01 – 0.03) magmatic	Replaced by cryptocrystalline aggregates of TiO_2 minerals, kaolinite, unidentified clay minerals (? smectites), pyrite and containing HFO minerals.
Pyrite	3 – 6 0.01 – 0.04 hydrothermal	Idiomorphic microcrystals finely disseminated only in reduced rocks.

TABLE 6-III (contd.).

Minerals	Vol.% Mean grain-size in mm Origin	Observations
Kaolinite	10 – 15 <0.01 hydrothermal (and supergene)	Replacement minerals of nepheline, alkali feldspars, aegirine-augite.
Unidentified clay minerals (? smectites)	tr. – 1 <0.01 hydrothermal (and supergene)	Replacement minerals of aegirine-augite.
TiO_2 minerals (? rutile)	tr. – 1 <0.04 hydrothermal	Replacement mineral of groundmass aegirine-augites, present as cryptocrystalline aggregates.
Sericite/illite	5 – 10 <0.02 hydrothermal	Replacement minerals of mainly nepheline/ kaolinite from nepheline.
Zircon	tr. 0.01 – 0.04 hydrothermal	Hydrothermal mineral sometimes altered to baddeleyite.
HFO minerals (limonite)	~5 <0.01 supergene	Clouded or rhythmically zoned distributions of cryptogranular aggregates forming pigmentations and impregnations. Only occurs in the oxidised rocks.
Microxenoliths	1 – 3 0.5 – >50 magmatic	Composed of angular fragments of phonolites and nepheline syenites of leucocratic to hololeucocratic composition included/ surrounded by a weakly flow-oriented RFI phonolite.

the same textures, except for the HFO minerals. The observations of pyrite dissolution and HFO mineral reprecipitation in the RFI rocks are in very good agreement with the descriptions and genetic interpretations of Blanchard (1968) which formed the basis for the discussion above.

4.3. X-ray diffraction (XRD) studies

Initial X-ray work was carried out at Paulo Abib Engenharia S.A., São Paulo, and completed using the equipment at the University of São Paulo (USP). Semiquantitative XRD analyses using LiF as an internal standard were run at the University of Bern by N. Waber. The XRD results of selected samples from RFI are shown in Table 6-IV. Textured preparations refer to powder preparations with planar orientation. Most samples were run in three laboratories, and with both planar and non-oriented powder preparations. The equipment at USP could only be used at 2 θ angles $\geq 5°$; therefore, smectite peaks could not be observed in these runs. In addition, for some samples, the analysed alkali feldspar peak (d ~3.25 Å) was more intensive than the chosen full scale deflection (of 1,000 cps). These peaks could not be measured and are therefore indicated in the table as not measurable (n.m.).

As the differences between duplicate runs (and runs made in different laboratories) were larger than the microscopically observed mineralogical variability, numerical (semi-)quantitative interpretations were avoided. The LiF (d ~2.01 Å) peak intensity (Table 6-IV) refers to an admixture (internal LiF standard) in the weight proportion 10:1 (10 samples, 1 LiF) and can serve as an estimate for the analytical conditions of these runs.

Some general conclusions from the X-ray results include the greater presence of smectites in the RFI samples than expected from the microscopic work (probably in the range of 3 – 6 vol.%). The latter indicated the presence of unidentified clay minerals (probably smectites) in trace amounts of 1 vol.% aggregated into pseudomorphs after aegirine-augites. The measured smectites are probably present as cryptocrystalline (submicroscopic) finely disseminated individual grains.

The illite/sericite (d ~10 Å) peak is always significantly weaker than the kaolinite (d ~7 Å) peak, supporting the relatively higher abundance of the latter mineral (Table 6-II). Complementing, and to some extent modifying, the microscopic results, one observes the highest kaolinite/illite peak intensity relationships and also the absolutely lowest illite peak intensities in the pitchblende nodules and bleached nodules. This

TABLE 6-IV
X-ray diffraction data of selected RFI samples.

Sample no. (split no.)	Run no.	Lab.	Preparation	Minerals: Peak heights (in mm) > background						Sample petrography
				Smectite d~15 Å	Illite d~10 Å	Kaolinite d~7 Å	Alk. feldspar d~3.25 Å	Uraninite d~3.10 Å	LiF d~2.01 Å	
RFI-I	I-A	PA	textured	11	12	37	n.m.	–	–	Oxidised bulk rock powders.
(1A)	I-A	USP	idem	–	9	17	135	–	–	
	I.3	Be	idem	6(?)	10	19	n.m.	–	48	
	I.3	Be	non-oriented	3(?)	8	12	140	–	38	
RFI-I	I-B	PA	textured	13	11	44	n.m.	–	–	Bleached nodule,
(1B)	I-B	USP	idem	–	8	22	210	–	–	selectively extracted
	I-1	Be	idem	7(?)	3(?)	16	190	–	32	powders.
	I.1	Be	non-oriented	10(?)	–	10	110	–	27	
	I.2	Be	textured	10(?)	3(?)	22	n.m.	–	41	
	I.2	Be	non-oriented	3(?)	2(?)	17	135	–	34	
RFI-II	II	PA	textured	9	15	28	n.m.	–	–	Reduced bulk rock (powder)
(2C)	II	USP	idem	–	14	24	137	–	–	adjacent to redox front.
	I.4	Be	idem	5(?)	4(?)	15	194	–	41	
	I.4	Be	non-oriented	–	8	13	108	–	34	
RFI-III	I.5	Be	textured	–	10(?)	21	176	–	45	Reduced bulk rock (powder)
(3B)	I.5	Be	non-oriented	4(?)	10	15	128	–	41	from centre of non-mineralised zone adjacent to the redox front.
RFI-III	III	PA	textured	3(?)	2(?)	8(?)	47	85	–	Pitchblende nodule of
(3C)	III	USP	idem	–	–	10	55	45	–	mineralised zone, selectively extracted.
RFI-IV	I.6	Be	textured	3(?)	–	12	88	70	29	Pitchblende nodule;
(4B)	I.7	Be	textured	2(?)	–	14	160	–	38	Reduced bulk rock (powder)
	I.7	Be	non-oriented	3(?)	3(?)	12	125	–	36	of mineralised zone adjacent to pitchblende nodule.

Abbreviations:
Lab = Laboratories
PA = Paulo Abib Eng. S.A.
USP = University of São Paulo
Be = University of Bern
n.m. = not measurable
– = not observed
(?) = uncertain peak identification

indicates that the U-oxide precipitation and dissolution, i.e. the pitchblende nodule formation and later destruction (with release of low pH sulphate concentrations), exercised some preferential attack on the mica mineral.

Alkali feldspars are the most abundant minerals of the RFI rocks and consist texturally of typical sanidine laths and prisms often of very fine grain-size (Table 6-III). Chemically, however, they are very pure K-feldspars (see section 6). These characteristics, together with the XRD patterns, indicate that crystal chemical exchange reactions affected the primary magmatic sanidines, substituting Na^+ for hydrothermal K^+ along with structural modification. These reactions produced the presently observed very pure K-feldspars of intermediate structural state and triclinicity (between high and low temperature). Similar processes were reproduced experimentally and confirmed using stable isotope studies by O'Neil and Taylor (1967) under P-T conditions that permit extrapolation/comparison with the "potassic rock" hydrothermal processes of Poços de Caldas (Waber *et al.*, this report).

The main U-minerals of the pitchblende nodules are cryptocrystalline U-oxides similar to those described by Barrington and Kerr (1961; referenced in the ASTM-index under No. 13-225) and others described by Swanson and Fuyat (1953). A comparison of the main X-ray peaks is shown in Table 6-V. The uraninite of the RFI pitchblende nodules, however, furnished broad X-ray lines indicating low crystallinity, probably allied with partial oxidation of the UO_2 to UO_3 (Table 6-V, column PH/HHW).

5. Rock physical parameters

Rock physical properties of RFI selected minor samples (see also section 6) and of the regional phonolites and nepheline syenites (Schorscher and Shea, this report series; Rep. 1) were determined by N. Waber (Univ. Bern). Results are shown comparatively in Table 6-VI. The measurements confirm the microscopic observations regarding the higher porosity of the oxidised RFI rocks when compared with the reduced non-mineralised rocks (Table 6-VI, sample no.: RFI-1A, B, C and RFI-5A, -6B; means 1 and 3).

Sample nos. RFI-4B and -3 are of reduced phonolites from (respectively) the zone of maximum U-mineralisation and the zone free of U-mineralisation due to dissolution adjacent to the redox front. They further support the results of the XRD studies which indicated that the supergene reducing processes of formation and subsequent dissolution

TABLE 6-V

X-ray diffraction data of uraninite from RFI pitchblende nodules compared to literature data.

a		b		RFI pitchblende		
d(Å)	Int.	d(Å)	Int.	d(Å)	Int.	PH/HHW
3.090	10	3.16	10	3.12	10	8.5
2.686	5	2.74	5	2.70	5	2.9
1.900	5	1.93	5	1.91	5	2.9
1.62	4	1.65	5	1.63	5	3.5
7 additional peaks down to d = 1.04 Å		5 additional peaks down to d = 1.05 Å		Interval not studied		

a = Midnite Mine (Barrington and Kerr, 1961)

b = Swanson and Fuyat (1953)

PH/HHW = Peak height to half height width ratio

of the pitchblende mineralisations occurred with partial silicate mineral replacement, causing a moderate elevation of the porosities (not observed microscopically).

Comparison of the RFI rocks with the regional rocks (Table 6-VI), for example in terms of their mean values (means 4 and 5), reveal strong differences in their global rock densities and porosities, even though they have identical grain densities. This indicates that the hydrothermal (reducing) potassic rock-forming and supergene (reducing and oxidising) processes compensated for the incurred porosity formation by precipitation of denser mineral phases such as pyrites in the reduced rocks and HFO minerals in the oxidised rocks. A graphic representation of the variation of the rock physical parameters of the RFI samples is shown on the scale profile of the redox front illustrated in Figure 6-2.

6. Geochemistry

6.1. Sample preparation and analysis

Two main representative sample sets were prepared for geochemical studies: one from large-sized homogeneous parts of the original samples and one from selected minor

TABLE 6-VI

Rock physical properties of selected RFI samples and regional alkaline rocks of the Poços de Caldas complex.

Sample no.	Density (Hg), global	Grain (solids) density	Porosity	Rock types
RFI-1A	2.17	2.62	17.1	RFI oxidised phonolite, ~20 cm from redox front;
RFI-1B	2.20	2.62	15.9	RFI oxidised phonolite, 15 to 5 cm from redox front;
RFI-1C	2.18	2.65	17.8	RFI oxidised phonolite, 5 to 0 cm from redox front, rich in HFO minerals;
RFI-3	2.17	2.64	17.8	RFI reduced phonolite, 0 to 10 cm from redox front, zone without U-nodules;
RFI-4B	2.20	2.61	15.5	RFI reduced phonolite (without U-nodules) of zone of max. U-mineralisation;
RFI-5A	2.35	2.59	9.4	RFI reduced phonolite, ~ 1 m from redox front (variety 1);
RFI-5B	2.26	–	–	RFI reduced phonolite, ~1 m from redox front (variety 2);
RFI-6B	2.33	2.61	10.6	RFI reduced nepheline syenite xenolith, ~2 m from redox front;
PDC-PH-02B	2.62	2.66	1.6	Regional nepheline syenite – hypabyssal;
PDC-I1-04	2.57	2.62	1.8	Regional phonolite – subvolcanic;
PDC-PH-05	2.59	2.61	0.6	Regional phonolite – volcanic;
PDC-I1-06	2.50	2.59	3.5	Regional nepheline syenite – plutonic;
PDC-I1-07	2.49	–	–	Regional nepheline syenite – plutonic;
PDC-PH-08	2.59	–	–	Regional phonolite – volcanic;
PDC-I1-01	2.55	–	–	Regional nepheline syenite – hypabyssal;
means 1	2.18	2.63	16.93	RFI oxidised rocks;
means 2	2.19	2.63	16.65	RFI reduced, mineralised and related rocks;
means 3	2.31	2.60	10.00	RFI reduced non-mineralised rocks;
means 4	2.23	2.62	14.87	RFI rocks, all;
means 5	2.56	2.62	1.88	Regional rocks, all.

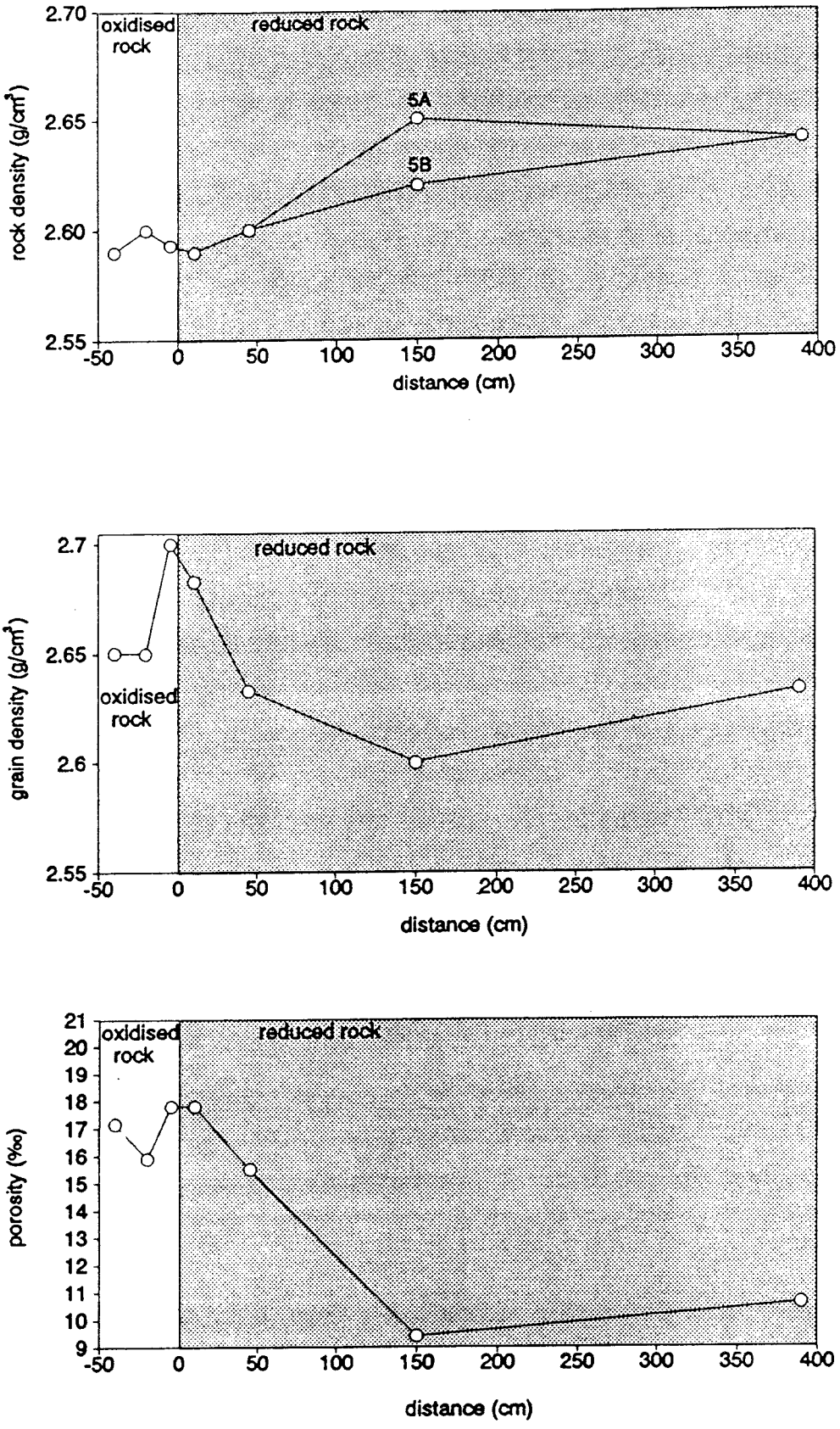

Figure 6-2. RFI redox front: distribution of rock physical properties.

portions cut out of the original samples (based on specific mineralogical, petrographic and metallogenetic characteristics). From these, as an additional detail, specific powder samples were removed by drilling for complementary geochemical (and mineralogical) analysis. Details of the different sample sets and the analytical work performed are presented in Tables 6-I and 6-II, and the chemical data are listed in Appendix 6:2.

Geochemical sample set I (Table 6-II) comprises five large-sized representative samples (750 – 1350 g) from the main mineralogical-petrographic zones of RFI. Major and trace element studies (by routine XRF analysis; University of Bern), determination of Fe^{3+}_{tot}, Fe^{2+}, S and Lost On Ignition (LOI) using classic methods, analysis of Mo by Atomic Absorption (AAS); work performed at Paulo Abib Engenharia S.A., São Paulo), and determination of Cd by AAS (work done by R. Mader, University of Bern) were carried out on the samples. Figures 6-4, 6-6 and 6-13 show the distribution of Fe^{3+}, S, LOI and Mo across the redox front. The geochemistry of Cd will be discussed later together with complementary data. Analytical problems arose during the determination of Fe^{2+}, probably due to the presence of uranium. Thus, even the reduced rocks with abundant pyrite showed below-detection-level amounts of FeO (<0.2 wt.%; Appendix 6:2; Table 6:2-I).

Geochemical sample set II (Table 6-II) comprises 10 samples selected from the original specimens in an attempt to further subdivide the main zones of the redox front, and also to consider the internal compositional and textural variations of the original samples. To accomplish this, the original sample RFI-1 was subsampled (1A, 1B, 1C) from the redox front (Table 6-II), progressing into greater HFO mineral contents as indicated by the more intensive yellowish-brown colouration.

The original sample RFI-4 was also subsampled (4A-1, 4A-2, 4B) to show different degrees of U-mineralisation. Sample RFI-4 represents the zone of maximum U-mineralisation and the subsamples prepared represent reduced types a) containing pitchblende micronodules (4A-1), b) devoid of macroscopically recognisable pitchblende nodules (4A-2), and c) of maximum U-content with abundant pitchblende macronodules (4B). Subsampling of RFI-5 resulted in sample 5A (non-mineralised) and 5B (contains pitchblende micronodules).

Sample RFI-6 was subdivided according to its lithological composition into sample 6A (reduced non-mineralised phonolite country rock) and 6B (reduced nepheline syenite xenolith). However, only 6B was analysed. The analytical results are presented in Appendix 6:2 (Table 6:2-II).

The mean geochemical variation of the respective elements in the regional (hydrothermally altered non-potassic) rocks, the borehole F1 reduced rocks and the

borehole F1 oxidised rocks were considered. Only in the case of Hf had comparative values for borehole F4 rocks to be used – i.e. oxidised phonolites and nepheline syenites (sample nos. 19-1A, 22-1A, 39-1A) and reduced nepheline syenite xenolith (sample nos. 413-1A-A; -1A-B; 1A-C; 1A-D; 1A-E), respectively, since borehole F1 rocks were not analysed for this element.

Concerning samples RFI-1A, -3B, -4B, -5B, and the S, Fe_2O_{3tot}, and LOI analysed by both laboratories (Paulo Abib Engenharia S.A., São Paulo and the University of Bern), one can see quite a good agreement of results, bearing in mind the different methods used and that the two sample sets were not homogenised splits, but simply from adjacent parts of the same original samples (Figs. 6-2, 6-6 and 6-4; Appendix 6:2, Tables 6:2-I and 6:2-II). This is particularly important in the case of sample RFI-4B, where the split analysed by the Paulo Abib laboratory was free of pitchblende nodules (analysis no. 06, Appendix 6:2; Table 6:2-I), in contrast to the split analysed by the University of Bern (analysis RFI-4B, Appendix 6:2, Table 6:2-II) which represented the maximum U-mineralisation, i.e. particularly rich in pitchblende macronodules (Appendix 6:1, Plate 6:1-4). This fact explains, for instance, the almost proportional differences in the Fe_{tot} and S results by a factor of 2.

6.2. Geochemistry of sample set I (large-sized samples)

Figures 6-6 and 6-4 show the stepwise and proportional decrease of S and Fe_{tot} from the reduced rocks (analysis no. 07; sample RFI-5B) towards the redox front (on its reduced side), corresponding, most probably, to the formation and partial removal in solution of Fe-sulphates from pyrite (even though dissolution of pyrite could not be positively confirmed microscopically). The mobilisation and release into solution of Mo (Fig. 6-13) is anomalous, apparently occurring as a continuous (one-stage) process in the near-vicinity of the redox front on the reduced side. This further supports the existence of specific Mo-minerals (probably sulphides) in the reduced rocks rather than its presence as a minor constituent (up to $\leq$ 1.500 ppm) in pyrite. However, it must be mentioned that molybdenite (MoS_2) has not been observed in the RFI rocks (either due to cryptocrystallinity or to its non-existence) and that the less likely jordisite (amorphous MoS_2) may in fact have been overlooked. In the field, one very frequently observes the presence of a blue Mo-mineral, most probably ilsemannite (Mo-hydrous oxide), in the presence of pyrite, i.e. only in the reduced rocks exposed to weathering. Ilsemannite is, according to Ramdohr (1975), most readily formed from the weathering of jordisite by

rapid oxidation (even in mineral collections). At the Osamu Utsumi mine the formation of the blue Mo-mineral was observed on drillcores of reduced rocks within time spans of only a few days. Jordisite is considered here as the more probable Mo-mineral phase in the reduced RFI rocks, even if the formation of the blue Mo-mineral in the studied rocks was not observed. With respect to jordisite being a paragenetic mineral forming part of the hydrothermal U-Zr-REE-mineralisation at the mine, there are some reservations. For example, jordisite is a very low temperature mineral (Ramdohr, 1975). From the oxidised side of a zone located outside the direct influence of the redox front, Mo-values may again reach up to half of the original content of the reduced rocks, and may have been fixed mineralogically by coprecipitation onto HFO-minerals of low crystallinity (mainly limonite).

6.3. Geochemistry of sample set II (main XRF samples)

The main major and trace element (XRF-) data-sets of the RFI redox front (Appendix 6:2; Table 6:2-II) are compared globally with other equivalent oxidised and reduced potassic rocks of the Osamu Utsumi mine, and with the regional rocks (unaffected by the potassic rock hydrothermal alteration) and related Zr-REE-U-mineralisation (Waber *et al.*, this report). In addition, the specific geochemical processes related with the development of the redox front are also discussed.

The XRF analytical data for RFI were recalculated to obtain mean values for the oxidised and reduced non-mineralised rocks (U $\leq$210 ppm) and for the reduced mineralised rocks (U >210 ppm). These are compared and related to one U-mineralised oxidised rock from the RFI front (U = 861 ppm, sample RFI-3), and to the mean values for borehole F1 oxidised and reduced rocks and the regional rocks (Appendix 6:2; Table 6:2-III). The non-mineralised reduced rocks were considered first, to try and reconstruct the character of the magmatic and superimposed hydrothermal geochemistries of the RFI rocks. It should therefore be remembered that these were initially classified mineralogically and petrographically as very fine-grained hololeucocratic volcanic phonolites containing subordinated phenocrysts of alkali feldspar, pseudoleucite, nepheline and aegirine-augite, and (micro-)xenoliths of phonolites and nepheline syenites, i.e. unsaturated alkaline rocks (section 4).

6.3.1. RFI phonolites: magmatic composition and hydrothermally altered potassic rock

Major elements

When comparing the major elements (and corresponding mean values) of the non-mineralised RFI rocks with the equivalent mean values for the reduced borehole F1 rocks (Appendix 6:2; Tables 6:2-II and 6:2-III), the similarities in TiO_2, Al_2O_3 and LOI contents, and the overall low and very low contents of Mn, Mg, Ca and P (-oxides), are easily observed. Differences include higher SiO_2 and K_2O contents in the RFI rocks and the higher Fe_2O_{3tot} and Na_2O contents of the borehole F1 rocks; Na_2O, in particular, is almost entirely absent in the RFI rocks. These differences are similar when compared to the equivalent borehole F4 rocks and to the redox fronts II, III and IV sampled and analysed by Waber *et al.* (this report; section 9).

In comparison with the regional rocks (Appendix 6:2; Table 6:2-III) it becomes evident that all the above observed differences (of the RFI and borehole F1 reduced rocks) not only continue to exist, but reach maximum values. Additionally, the regional rocks also show minor but significant MnO and MgO contents and much lower LOI. If the RFI reduced non-mineralised rocks are plotted together with the regional rocks in a total alkali-silica (TAS) diagram (Le Maître, 1984) and compared with the borehole F1 rocks (Waber *et al.*, this report), all rocks are observed to lie in the phonolite (unsaturated) field. The RFI rocks, however, plot near the divide with the field of more (silica) saturated rocks (alkali trachytes and trachytes), in contrast to the regional rocks which plot in the opposite, more unsaturated part of the phonolite field. The borehole F1 rocks cover the main part of the phonolite field and the calculated means of the reduced non-mineralised varieties lie at the centre. Bearing in mind the reconstructed magmatic mineralogy of the RFI rocks (see section 4; Table 6-III) and the chemistry of the mineralogically similar regional rocks (particularly of the regional phonolites), it becomes evident that the original RFI rocks were certainly more leucocratic (Fe-Mg mineral poor) and their chemical composition is mainly a product of the "potassic rock" hydrothermal alteration. This imposed on the original rocks the progressive and ultimate total loss of Na_2O, the equally complete loss of CaO, MnO and MgO, and the partial loss of Fe_2O_{3tot} (while the preserved Fe was almost completely reduced to the divalent state and reprecipitated mainly as pyrite). The Na_2O loss was not entirely compensated by the addition of K_2O; there also occurred moderate to substantial enrichments of SiO_2 and Al_2O_3, whereupon nephelines underwent partial alteration to illite/sericite and kaolinite (causing SiO_2 and K gains, but total-alkali losses at ~ constant Al_2O_3) and the main

magmatic sanidines suffered alkali exchange reactions (Na by K), structural readjustments, and incipient kaolinisation (which caused increases in K and Al_2O_3 and important Na and minor SiO_2 loss). The almost total loss of CaO, MgO and MnO, and the partial loss of Fe_2O_{3tot}, are explained by the argillation of magmatic Fe-Mg minerals, mainly of aegirine-augites, through the formation of pseudomorphs comprising mixtures of clay minerals (kaolinite, smectite), pyrite and Nb-Fe-rutile (with consequent losses in variable proportions of Na, Ca, Mg, Fe, Mn, Si). Possibly, there also occurred the dissolution of minor magmatic plagioclase feldspar and of the minor anorthite components of ternary magmatic (alkali-) feldspars.

TiO_2 is present in the RFI and borehole F1 rocks in similar amounts, somewhat lower, however, than in the regional rocks. Magmatic Ti occurs in these rocks in rare oxidic ore minerals, but mainly as a minor element in the clinopyroxenes. (Giannettite is a pneumatolytic Ti-bearing mineral of the regional rocks, hydrothermally unstable, but less frequent in phonolites.) These have been generally referred to as aegirine-augites, but even the groundmass clinopyroxenes of the volcanic phonolites show compositional zoning. This is particularly well developed in the case of the coarser phenocrysts and nepheline syenite regional rocks (Schorscher and Shea, this report series; Rep. 1), ranging from sodi-augitic centres to almost pure aegirine rims. Ulbrich (1983) and Ulbrich *et al.* (1984) reported microprobe analyses of the clinopyroxenes of various nepheline syenites from Poços de Caldas with TiO_2 contents ranging from 0.5 wt.% in the centres to 5 wt.% at the aegirine borders. Due to its geochemical immobility, Ti reprecipitates (hydrothermally) in situ as TiO_2- (rutile-) minerals, pseudomorphing the clinopyroxenes.

Minor and trace elements

To discuss the original magmatic and superimposed hydrothermal trace element geochemistry of the RFI non-mineralised, reduced phonolites is more problematic, even if the equivalent borehole F1 rocks are also included for comparison (Appendix 6:2; Tables 6:2-II and 6:2-III). For instance, the trace element geochemistry of the borehole F1 rocks (Waber *et al.*, this report) showed that macro- and microscopically they are very similar, and that in the core profile more or less contiguous rocks showed abrupt differences in their trace element contents, in some cases by factors of 2 to >10. This has a major influence, for instance, upon mean values, even in the case where quite a high number of analysed samples are petrographically similar. In the case of RFI, and similarly with the RFII, III and IV redox fronts, the numbers of analysed samples are

relatively low and the interval between the individual samples comparatively high. The occurrence and influence of individual samples of anomalous geochemistry in these types of populations is evidently possible and marked. Therefore, to avoid misinterpretation, the nature/origin of these geochemical anomalies in the redox front samples, i.e. whether primary-magmatic, hydrothermal or redox front-related supergenic, must initially be well characterised.

For RFI samples, RFI-3, RFI-4A-2, RFI-5A and RFI-6B (Appendix 6:2; Table 6:2-II) were considered to represent the mean composition of the reduced non-mineralised (U <210 ppm) RFI rocks (Appendix 6:2; Table 6:2-III). However, even though microscopically the first three (phonolite) samples can be considered as similar, the fourth sample, a nepheline syenite xenolith, was also included, even though of different chemistry. Only in the case of Ba were two mean values calculated for both RFI (reduced non-mineralised) and regional rocks: one comprising all the rocks (nepheline syenites and phonolites), the other only the phonolites.

The RFI reduced non-mineralised rocks are compared to the equivalent borehole F1 rocks and to the regional rocks in order to establish their possible primary magmatic and hydrothermal trace element geochemical characteristics (Appendix 6:2; Table 6:2-III).

Elements Ba, Rb, Th, U, V and Zn

These elements are systematically enriched in the reduced, non-mineralised RFI and borehole F1 rocks, when compared with the regional rocks. In the case of Ba, two mean values are given for RFI and regional rocks (Appendix 6:2; Table 6:2-III). The initial (higher) means include in both cases all the rocks (phonolites and nepheline syenites) and the second only the extremely fine-grained, volcanic phonolites. This was necessary because, in the case of the regional rocks, there exists a very characteristic, strong fractionation of Ba between the fine-grained phonolites (means: 50 ppm) and the coarse-grained nepheline syenites of hypabyssal to subvolcanic and plutonic origin (means: 387 ppm). Similarly, in the case of the RFI rocks, the nepheline syenite (Appendix 6:2; Table 6:2-II; sample RFI-6B) has a much higher Ba content than the means of the associated volcanic phonolites. Therefore in this case, the means of the RFI volcanic phonolite are considered more representative and should be compared with the equivalent means of the regional phonolites for the appropriate estimation of the Ba-enrichment factor. For the RFI and regional phonolites this is ~7.

Such evident fractionation was only observed in the case of Ba. Furthermore, the petrographic variability of borehole F1 shows that it includes predominantly subvolcanic

to hypabyssal rock types, and only minor well-defined plutonic and shallow volcanic rock types. Therefore, the mean values for all the rocks, rather than the partial means from minor lithological subgroups, were used for the other comparisons, including Ba from the borehole F1 and regional rocks. Its enrichment factor in this case is lower (~2.5). One mineralogical reason for the enrichment of Ba in the hydrothermally altered rocks could be the inclusion of a complementary celsian component during the alkali exchange reactions of the feldspars. This interpretation is supported by Ulbrich (1983) and Ulbrich *et al.* (1984) who have described the erratic presence of low Ba contents, similar to those of CaO ($\leq$0.36 wt.%), in the alkali feldspars of nepheline syenites from Poços de Caldas. In addition, barite is known in hydrothermally altered rocks from the Osamu Utsumi mine, and its existence as a minor finely-dispersed mineral in these rocks could not be totally excluded.

The enrichment of Rb by a factor of 1.7 in RFI and 1.9 in the borehole F1 rocks corresponds quite well to the K_2O enrichment factors (1.7 and 1.6 respectively). This process, too, is mineralogically related to the hydrothermal alkali exchange reactions of the feldspars and, to a lesser extent, to the hydrothermal sericite/illite formation in the pseudomorphs resulting from nepheline.

Thorium has higher mean values in the RFI and borehole F1 rocks than in the regional varieties. The borehole F1 mean value, moreover, lies within the range of data published from various global alkaline intrusive complexes (Roger and Adams, 1978). However, based on the few analysed regional rocks in the Poços de Caldas complex it is difficult to decide whether the Th means of borehole F1 really represent a weak hydrothermal enrichment, or whether the Th mean value of the regional rocks represents unusually Th-poor rocks. The RFI rocks are quite clearly Th-enriched with respect to the borehole F1 rocks by a factor of 2, and to the regional rocks by a factor of 6. The attempt to correlate Th with another trace element for the four individual RFI samples yielded at best a reasonably good positive linear correlation with Zr. If the borehole F1 and regional rock mean values are included, they lie quite close to each other, but are still totally isolated from the correlation line.

This tends to indicate that the Th-contents of the borehole F1 rocks probably represent low or unmodified magmatic values, while those of the RFI reduced non-mineralised rocks are of hydrothermal origin. Specific Th-minerals were not observed. Microprobe analysis of hydrothermal zircons from the borehole F1 rocks indicated the presence of Th in zircons from the potassic rocks of the mine (Waber *et al.*, this report, Appendix 3). Giannettite, however, is the main Zr-bearing mineral in the regional rocks.

Uranium is enriched in both RFI and borehole F1 rocks in relation to the regional rocks, where the U-content was consistently below the XRF detection limit (<5 ppm); the respective mean values for the RFI and borehole F1 reduced non-mineralised rocks are 146 and 32 ppm U. No systematic variation and/or correlation of U with other elements could be observed from the RFI means. Therefore, the higher U-enrichment of the RFI rocks compared to the borehole F1 rocks is considered to be due to complex processes related to superimposed hydrothermal and reducing redox front mechanisms. The borehole F1 means are considered to represent the mean U-content of the reducing hydrothermal potassic rock-forming process, and not the associated higher grade U-mineralisation. Higher grade, truly hydrothermal (deep- seated) U-mineralisations were only analysed recently in samples from borehole F4. These were found to consist of minor U-oxides associated mainly with zircon, baddeleyite and pyrite (Waber *et al.*, this report; Appendix 1). Analyses show mostly a positive U – Zr correlation, even though there were some variable correlation factors in each of the studied examples. This may indicate the inhomogeneity of the hydrothermal U-mineralising fluids that acted in restricted locations at the Osamu Utsumi site during the more general hydrothermal alteration which gave rise to the potassic rocks.

Specific U-minerals were not identified in the studied RFI and borehole F1 rocks, although it is believed that finely dispersed rare U-oxides may be present. Vanadium shows a mean value of about 70 ppm in the regional rocks, where it is bound to the aegirine-augites. The mean V values of the RFI and borehole F1 reduced, non-mineralised rocks (about 3 times that of the regional rocks) are practically identical with one another. Thus, V has not only an early magmatic origin, but can also be related to the hydrothermal potassic rock-forming process, independent of the grade of U-mineralisation. Specific V-bearing minerals were not identified in the RFI or borehole F1 rocks although they may be present in minor or trace amounts in the sericites/illites.

Zinc shows a somewhat similar behaviour to V; it already occurs in quite high amounts in the regional rocks (means of 168 ppm), bound to the silicate minerals (mainly pyroxenes). In the course of the hydrothermal alteration it becomes enriched, attaining practically identical mean values (about 220 ppm) in the RFI and borehole F1 rocks. Here it is present as fine sphalerite; no relationship with the U-mineralisation was observed.

Elements Sr, Pb, Nb, Zr, Ga and Hf

Strontium occurs in the regional rocks in concentrations typical for worldwide nepheline syenites (1,000 – 3,000 ppm; Goldschmidt (1954)), with a mean content of 1,913 ppm. Much lower contents and mean values are found in the hydrothermally altered (non-mineralised) RFI (626 ppm) and borehole F1 rocks (181 ppm), being reduced respectively by factors of ~3 and >10. Similarly, lower Sr mean values (than those of the regional rocks) are found in the borehole F4 reduced (non-mineralised) rocks and in the RFII, III and IV reduced non-mineralised rocks. The hydrothermal Zr – U– REE mineralised rocks of borehole F4 may achieve higher Sr contents than the regional rocks, thus showing that an Sr-enrichment occurred during the high-temperature hydrothermal mineralising processes. However, the Sr enrichment factors vary strongly, not only between different occurrences but also within individual mineralised zones.

The redox front-related U-mineralisations show no relationships with Sr. It is known that the typical alkaline (magmatic) minerals of feldspathoidal (alkaline) rocks such as nepheline, leucite, orthoclase and sanidine may contain quite high amounts of Sr (Goldschmidt, op. cit.). Ulbrich (op. cit.) and Ulbrich *et al.* (op. cit.) confirmed SrO contents of up to ≥ 1 wt.% in nepheline syenite alkali feldspars from Poços de Caldas. Sr contents are lower in the case of equivalent hydrothermal minerals, for instance in low-temperature K-feldspars or in mica minerals resulting from the replacement of feldspathoids. This may explain the observed reduction of Sr in the studied RFI and borehole F1 rocks as being due to the associated processes of low-temperature (hydrothermal) alkali exchange reactions of the feldspars and the replacement of feldspathoids. The differences between RFI and borehole F1 rocks (and the other reduced non-mineralised rocks) are thought to reflect primary magmatic variations.

Lead occurs in very low concentrations near, or even below, detection level (<6 ppm), in both the regional (non-altered) and borehole F1 reduced (non-mineralised) rocks; higher contents (mean value = 47 ppm Pb) were found in the RFI rocks. These may be related to the magmatic and hydrothermal variations, but also, at least in part, to the higher U-contents of the studied RFI rocks. No Pb or Pb-bearing minerals were found in the discussed rocks. The occurrence of galena associated with the hydrothermal U-mineralisation has been mentioned in Urânio do Brasil internal reports, but has not been confirmed in this study of the high-grade hydrothermal U-mineralisation.

Niobium occurs in the regional rocks in normal concentrations (mean: 249 ppm) for alkaline rocks of these types, and also shows similar concentrations in the borehole F1

(226 ppm) and RFI rocks (277 ppm). In the regional rocks, Nb is thought to substitute mainly for Ti in the magmatic clinopyroxenes and probably in giannettite as well. In the hydrothermally altered rocks (borehole F1 and RFI) it is known to occur in the TiO_2-(rutile-)minerals that form complex pseudomorphs after clinopyroxenes (Waber *et al.*, this report; section 5). In the borehole F1 rocks an almost perfect correlation of Ti and Nb can be observed (Waber *et al.*, op. cit.).

Zirconium and hafnium will be discussed together. The former shows similar mean concentrations (of 965 and 929 ppm respectively) in the regional and borehole F1 rocks, reduced by about half in the RFI rocks (means = 445 ppm). Hafnium was only analysed in the regional and RFI rocks, showing practically identical concentrations of 12 and 11 ppm. Hafnium is well known to substitute for Zr in Zr-minerals, but the main Zr-mineral species in the studied rocks are very different, consisting of giannettite in the regional rocks and zircon in the borehole F1 and RFI rocks. This, and the fact that hydrothermal zircons are normally richer in Hf than their magmatic equivalents, may explain the differences in the Zr/Hf ratios of the regional rocks (~80) and the RFI rocks (~40). Microprobe analysis of hydrothermal zircons of the borehole F1 reduced rocks showed consistently the presence of 1.0 – 1.5 wt.% of HfO_2. The low total Zr contents in the RFI rocks, when compared with more than double the amount of Zr in the borehole F1 and regional rocks, are considered to be relicts of the primary magmatic geochemical character of the RFI phonolites.

Gallium was analysed only in the RFI and borehole F1 rocks, where it occurs in mean concentrations of 37 and 22 ppm in the reduced non-mineralised varieties. These are in fact low concentrations for nepheline-alkali feldspar rocks (Goldschmidt, op. cit.). As Ga analyses of the regional rocks of Poços de Caldas were not performed (and are unknown from the literature), the low contents of this element in the hydrothermally altered rocks (that tend to be richer in Al than the regional rocks and should therefore be also richer in Ga) are considered indicative either of the existence of alkaline magmas anomalously low in Ga at Poços de Caldas, or of a specific type of hydrothermal reducing alteration that enriched Al but leached Ga from the non-mineralised RFI and borehole F1 rocks.

Some rare-earth (REE) and related elements: La, Ce, Nd, Y, Sc

Routine XRF analyses do not yield very precise results for the REEs. These data should therefore be treated as semiquantitative and should only be used for the relative comparison of mean values.

In the regional, borehole F1 and RFI rock groups, the REE (mean) contents follow the natural sequence of abundance: Ce followed closely by La and, to a lesser extent by Nd. In addition, the total abundances of these elements in the regional and borehole F1 reduced non-mineralised rocks are quite similar (most probably lying within the limits of analytical uncertainties). In contrast, the RFI (reduced non-mineralised) rocks show individual and mean values significantly lower than those above (Appendix 6:2, Table 6:2-III); La and Ce are reduced by at least 5 to 6 times and Nd by more than 10 times.

The light REEs, La, Ce and Nd are expected to be fixed in the regional rocks in the clinopyroxenes, alkali feldspars and Zr-minerals (mainly giannettite). In the reduced borehole F1 rocks they are associated with the hydrothermal zircons (mainly Ce); however, in the hydrothermally exchanged alkali feldspars La, Ce and Nd are, if present at all, below the microprobe detection level (estimated ≤ 500 ppm).

The correlation of La, Ce and Nd with Zr is evident for the three compared groups, particularly if the analytical uncertainties are kept in mind. If the geochemical immobility of REEs is also considered, it may be concluded that the RFI phonolites were, in terms of their magmatic origin, strongly depleted in REEs (La, Ce and Nd), as they were in Zr. The hydrothermal reducing potassic rock alteration heat, judging from the comparison of regional and borehole F1 rocks, shows that only a very minor effect on these elements occurred, if at all.

Yttrium is similar to the REEs in showing the same concentrations in the regional and borehole F1 rocks, but is about 2 times less in the reduced non-mineralised RFI rocks. Yttrium should also be present in the regional rocks, mainly in the clinopyroxenes, and possibly in giannettite (and other rare metal silicates). In the borehole F1 rocks Y is most frequently found in crystallo-chemically significant amounts in zircons and zircon-baddeleyite intergrowths (Waber *et al.*, this report, section 5). This, however, would imply higher Zr-contents in the RFI rocks (where in fact they are diminished) or, alternatively, higher Y-contents in the RFI zircons. As such indications are however lacking, it is thought that the higher Y-contents of the RFI reduced rocks may somehow be related to their higher U-content. It is known that various hydrothermal U-mineralisations formed by alkali metasomatism are also associated with Y and heavy REE enrichment (for instance: Porto da Silveira, 1986; Porto da Silveira *et al.*, 1989).

Scandium was only analysed in the regional rocks and borehole F1 rocks. In the former, the mean values are below the XRF detection limit (<1 ppm), and in the borehole F1 reduced, non-mineralised rocks a value of 2 ppm was obtained. These very low values are within the expected limits for nepheline syenites (Goldschmidt, op. cit.).

Elements Cr, Ni, Co, Cu, F and S

Cr, Ni, Co and Cu occur in the three rock groups in very low amounts, near or even below the XRF detection limit (Appendix 6:2; Table 6:2-III). Even Co, which in various hydrothermal U-occurrences is one of the typical elements, occurs in higher amounts at the Osamu Utsumi mine in only one (of the studied) hydrothermally mineralised intersections of borehole F4. In the RFI rocks all of these elements show very low total concentrations, which precludes any further interpretation.

Fluorine was analysed only in the regional and borehole F1 rocks with similar results (within the limits of analytical uncertainty). In the borehole F1 reduced non-mineralised rocks, F is most commonly present as rare fluorspar and may also still be a minor constituent in the hydrothermal white micas (sericite/illite). Fluorspar is also known from late pegmatitic to autohydrothermal veins of the regional rocks. Besides, F may be present in minor amounts in aegirine and giannettite and other rare metal silicates of the woehlerite group.

Sulphur as the sulphide ion is one of the important elements of the hydrothermal potassic rock (reducing) processes at the Osamu Utsumi site. It is typically high in the reduced RFI and borehole F1 rocks, where it is bound to the sulphidic ore minerals pyrite, sphalerite, (?)jordisite, (?)greenockite and others. The regional rocks are poor in S, where it should be present in cancrinite, sodalite and nosean.

Conclusions

In conclusion, the RFI non-mineralised reduced phonolites must be considered as being derived from the original magmatic rocks that were typically low in Zr and La, Ce and Nd. Otherwise the trace element compositions for these types of unsaturated hololeucocratic nepheline- and pseudoleucite-bearing rocks are normal. The hydrothermal reducing potassic rock alteration led to the enrichment of Ba, Rb, V, Zn and S, independent of the grade of U-mineralisation. The enrichment of Th, Pb, Y, Zr and U occurred as both a direct and indirect consequence of the associated (hydrothermal) mineralising processes. In the case of U, some redox front-related supergenic-reducing enrichment also probably occurred. Strontium was lost in the course of hydrothermal alteration and Nb and Hf maintained concentration levels similar to those of the regional igneous rocks. The Zr/Hf ratio is however less in the RFI rocks due to their lower total Zr content and to their particularly Hf-rich hydrothermal zircons. Scandium, Cr, Ni, Co and Cu occur in very low total concentrations in both the regional magmatic and the hydrothermally altered RFI and borehole F1 rocks; this is considered

normal. Gallium and F were not analysed in the regional magmatic and the RFI rocks. The former shows concentrations lower than normal for magmatic nepheline-alkali feldspar rocks in the hydrothermally altered rocks, and the latter shows similar concentrations when compared to the borehole F1 and regional rocks.

6.3.2. RFI oxidised and reduced phonolites

The non-mineralised reduced RFI and borehole F1 rocks are compared here with the equivalent oxidised RFI and borehole F1 rocks. Comparisons are based on the mean values obtained for a total of 16 analysed individual samples (Appendix 6:2; Table 6:2-III) including the RFI rocks from samples RFI-1A and RFI-1B and the borehole F1 rocks.

Comparison of the major elements shows only minor systematic variations that include increasing Al_2O_3 (and possibly TiO_2 and K_2O contents) in the oxidised rocks; SiO_2 diminishes very slightly and LOI more characteristically. Calcium, if present in the reduced rock, is almost totally eliminated. Among the other elements, Fe_2O_{3tot} shows insignificant variation and MnO, MgO and P_2O_5 maintain very low concentration levels. This is also the case for Na_2O in the RFI rocks. The apparent enrichment of Na_2O in the borehole F1 oxidised rocks is erroneous; the higher contents are due to the preservation of less altered perthitic K-feldspars in some of the oxidised rocks (Waber *et al.*, this report; Appendix 4).

These major element variations between reduced and oxidised RFI (and borehole F1) rocks may be largely explained by incipient oxidising lateritic weathering processes producing further kaolinisation (Al_2O_3-increase, SiO_2-decrease), pyrite oxidation (LOI reduction), HFO mineral precipitation (irregular Fe_2O_{3tot} redistribution), possible carbonate and fluorite dissolution (CaO decrease), and rock-solid volume reduction and residual enrichment of K_2O (in weathering-resistant white micas) and TiO_2 (in rutile/hydrorutile minerals).

In comparison, the trace element variations show systematic but minor enrichments of Rb, partial depletion of Sr, strong depletion of Zn and S, and significant enrichment of Ga in the oxidised rocks. The REEs, La, Ce and Nd, were inert/immobile during the oxidising supergenic process. Ba and Nb show non-systematic variations and V is immobile, or only very slightly enriched, in the borehole F1 rocks, but strongly enriched in the RFI oxidised rocks.

Cr, Ni, Co, Cu and Sc (analysed only in the borehole F1 rocks) maintain very low total concentrations and F, analysed only in the borehole F1 rocks, is significantly diminished in the oxidised rocks.

Pb, Th, U, Y, Zr and Hf in the RFI rocks behaved differently from those in the borehole F1 rocks due to the higher grade of U-mineralisation of the former. Upon oxidation, a drastic reduction of Zr in the RFI rocks, and a consequent reduction of Hf, Y and Th, were also observed; similarly a decrease of U and Pb occurs.

In the borehole F1 rocks Zr and Y were generally immobile, and Pb, Th and U show higher concentrations in the oxidised than in the reduced rocks. However, the total concentrations of Pb, Th and U are within the range of these elements present in the oxidised RFI rocks.

The observed trace element variations further support the major element results, i.e. Rb enrichment is sympathetic with K_2O, Sr depletion with CaO; Zn and S indicate the dissolution/oxidation of sphalerite and of all the other sulphide minerals. The enrichment of Ga is, as that of Al_2O_3, typical for lateritic weathering. This is confirmed by the immobility (within the restrictions of analytical uncertainties) of the REEs and also Ba and Nb, and by the enrichment of V.

Cr, Ni, Co, Cu and Sc are known to become enriched during lateritic weathering; however, their low availability during the incipient stages of the process may have resulted in their chemical uniformity. The decrease of F in the oxidised borehole F1 rocks is confirmed by the mineralogy, which points to the total dissolution of fluorite during oxidation of the rock.

Pb, Th, U, Y, Zr and Hf behave differently in the RFI and borehole F1 rocks. In the former, their behaviour corresponds to weathering dissolution with partial laterite reprecipitation of a hydrothermal low-grade radioactive mineralisation. This has also resulted in the partial dissolution of ZrO_2 – HfO_2-rich, Th- and Y-bearing hydrothermal zircons, and in the partial dissolution of (probably) U-oxide minerals and of (radiogenic) Pb. In the case of the borehole F1 rocks, Zr and Y remained inert and Pb, Th and U enrichment occurred from the considerably lower "protore" levels of the reduced rocks, to what may be considered the initial stages of their concentration, to form a lateritic geochemical anomaly in the oxidised rocks.

6.3.3. RFI redox front processes

Major and trace elements (XRF data)

The geochemical character of the RFI redox front is shown in Figures 6-3 to 6-13, and will be briefly discussed in comparison with the RFI non-mineralised, reduced and oxidised rocks mean values.

Four U-mineralised samples were included with the analysed RFI rocks. One (RFI – 1C) typifies an oxidised U-mineralised zone directly adjacent to the redox front (of about 5 cm width). The others are from reduced samples RFI-4 and RFI-5; of these samples RFI-4A-1 and RFI-4B represent the zone of maximum U-mineralisation and samples with weak U-mineralisation respectively. Mineralisation is in the form of pitchblende micro- and macronodules. RFI-5B also represents a weakly mineralised sample with pitchblende micronodules, but its relationship to the redox front is not known and is therefore considered anomalous.

The oxidised U-mineralised zone (sample RFI-1C) shows, among the major elements (relative to the mean values of the respective RFI oxidised and non-mineralised rocks), a slight decrease in SiO_2 and an increase in Fe_2O_{3tot} and LOI values. Of the trace elements, Zn, Co, Ni, La, Ce, Nd, Pb and, particularly strongly, U and S tend to be concentrated in the mineralised zone. Of the remainder, Y was slightly depleted and V enriched (but less than the means of the oxidised rocks) and the other elements remained within or very near to their mean values. Specific mineral phases that may be related to the observed geochemical anomalies could not be detected, except for HFO minerals (mainly limonite). These are known to coprecipitate available metals, e.g. REEs and U in lateritic deposits, but they do not explain the high S content. It is thought that possibly jarosite or similar Fe^{3+}-sulphates may also have formed, accounting for the S and trace element abundances (Bambauer *et al.*, 1988, 1989).

Of the redox fronts sampled and analysed by Waber *et al.* (this report), only RFII (in volcanic breccia) showed a comparable oxidised Fe – U – S enrichment, directly adjacent to the redox front. This and sample set I, without an oxidised U-mineralised zone (Figures 6-4 and 6-6), seem to indicate that the development of such a zone is either not a general feature of the redox fronts, or is restricted to very narrow zones (note that sample RFI-2B of sample set I is a few cm more distant from the redox front than sample RFI-1C of set II).

The reduced, non-mineralised zone directly adjacent to the redox front on the reduced side (sample RFI-3B) shows only weak geochemical variations when compared to the reduced non-mineralised rock. Al_2O_3, TiO_2, Ga, V and Pb are enriched and Zr, Y, Th,

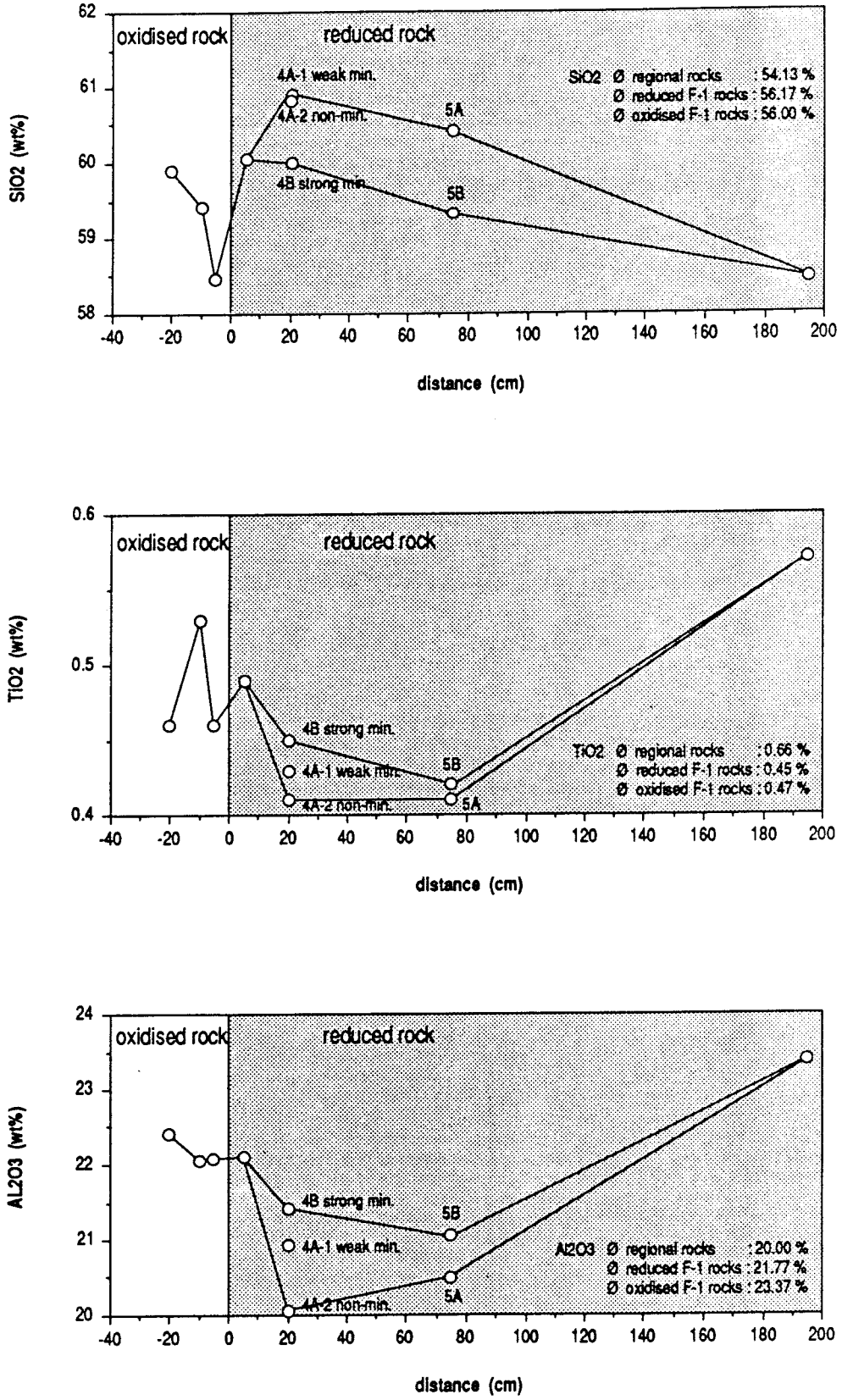

Figure 6-3. RFI redox front: geochemical distribution of selected elements/parameters.

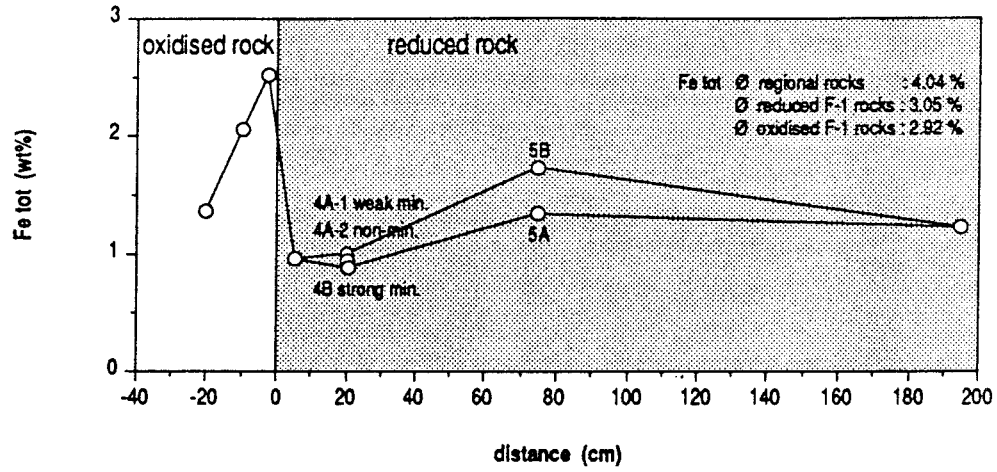

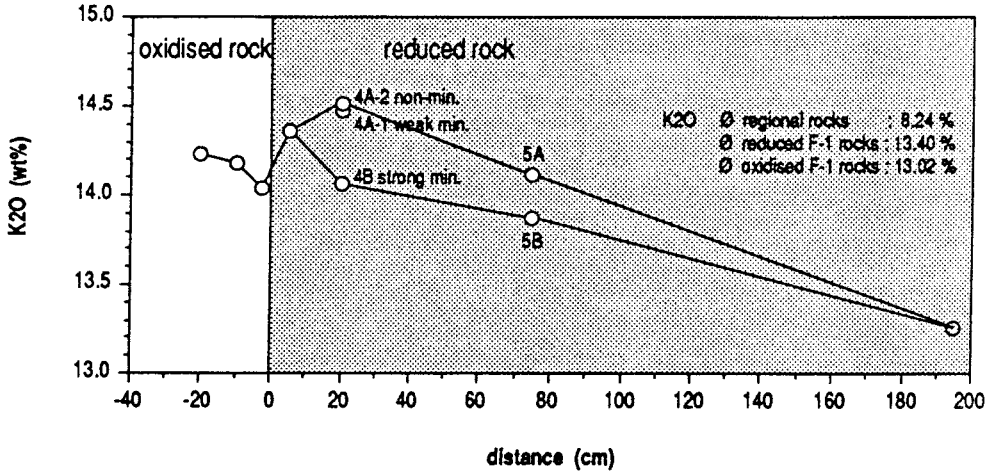

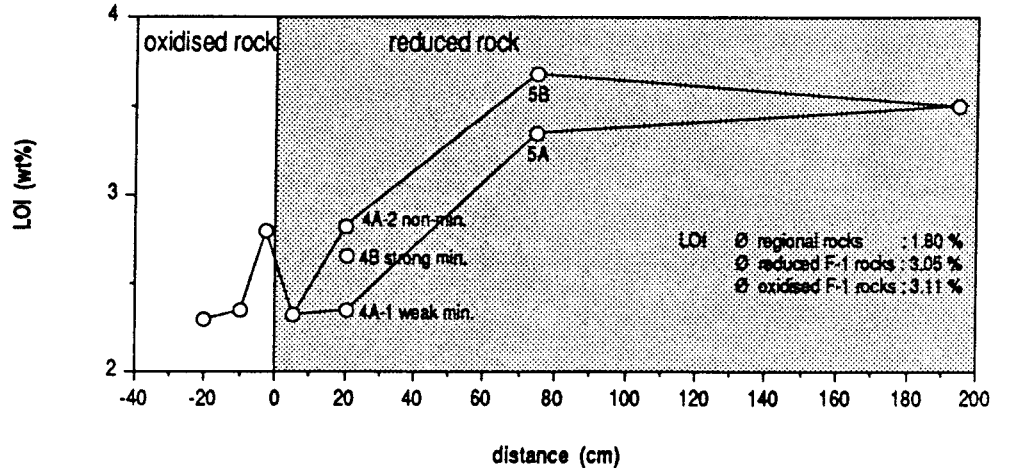

Figure 6-4. RFI redox front: geochemical distribution of $Fe_2O_{3(tot)}$, K_2O and LOI.

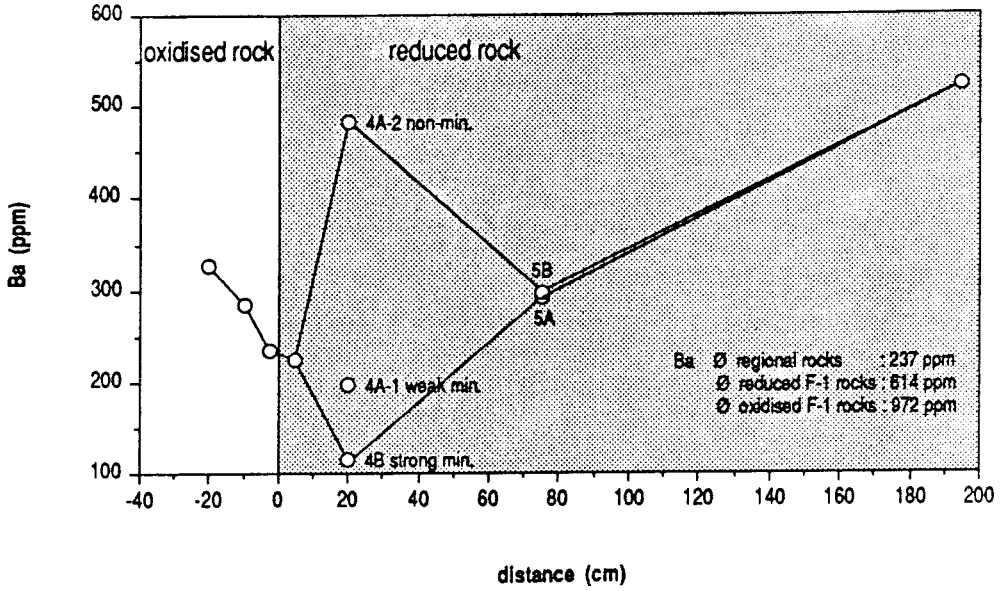

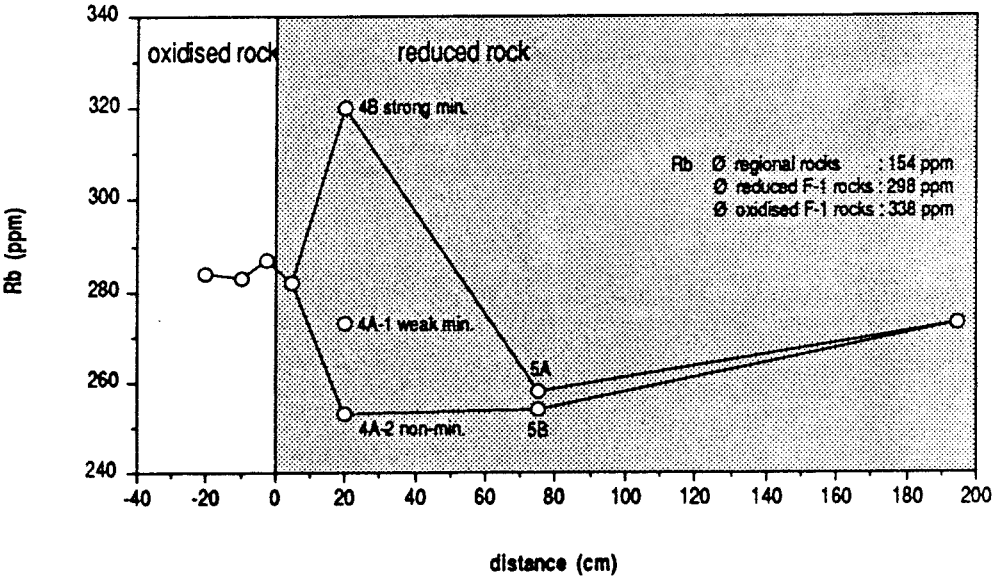

Figure 6-5. RFI redox front: geochemical distribution of Ba and Rb.

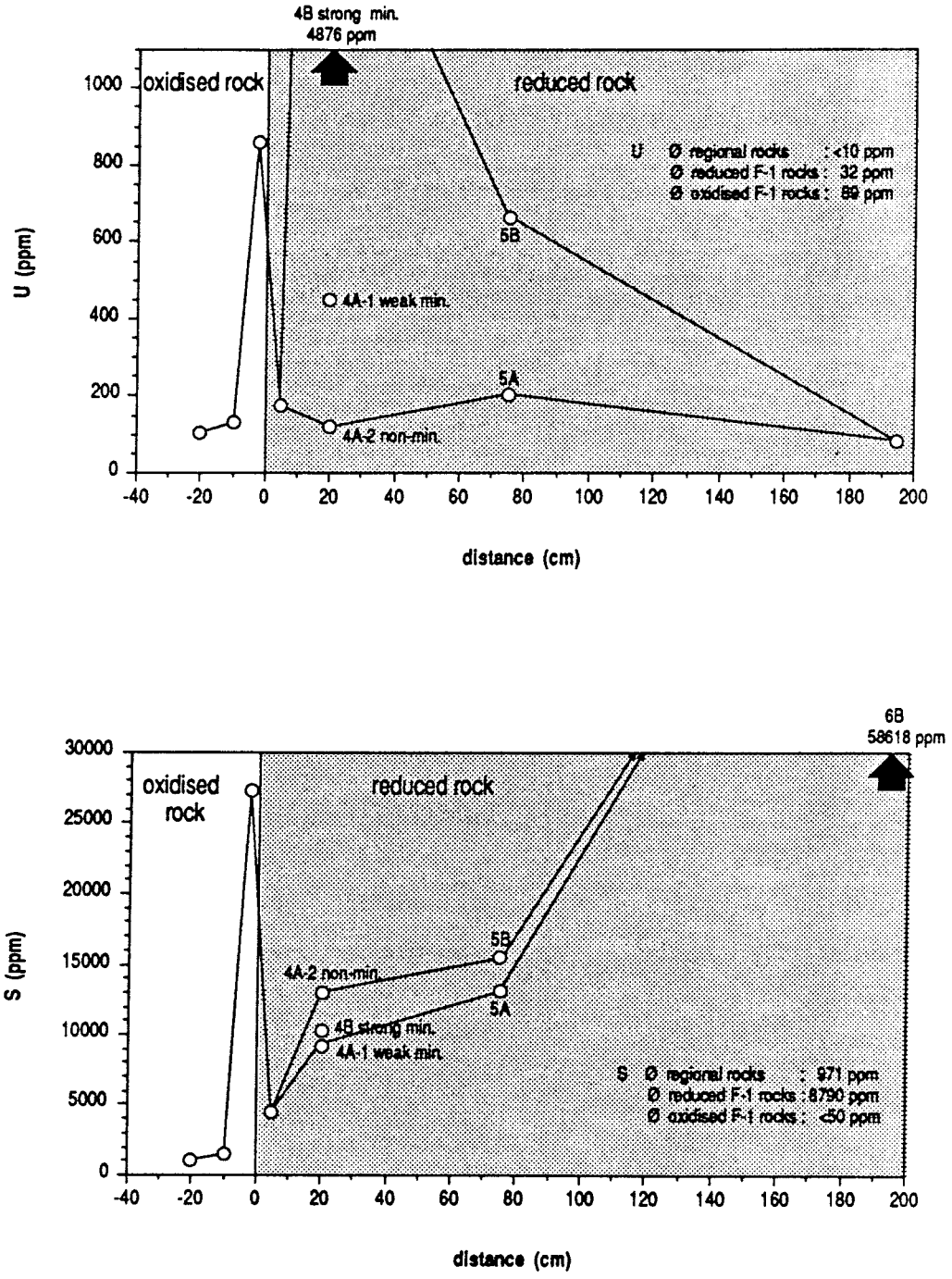

Figure 6-6. RFI redox front: geochemical distribution of U and S.

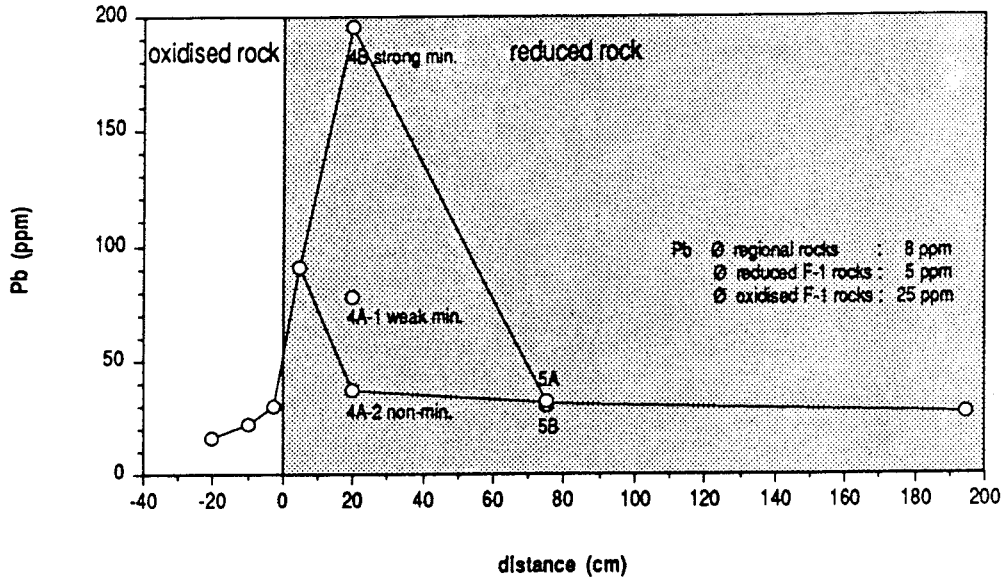

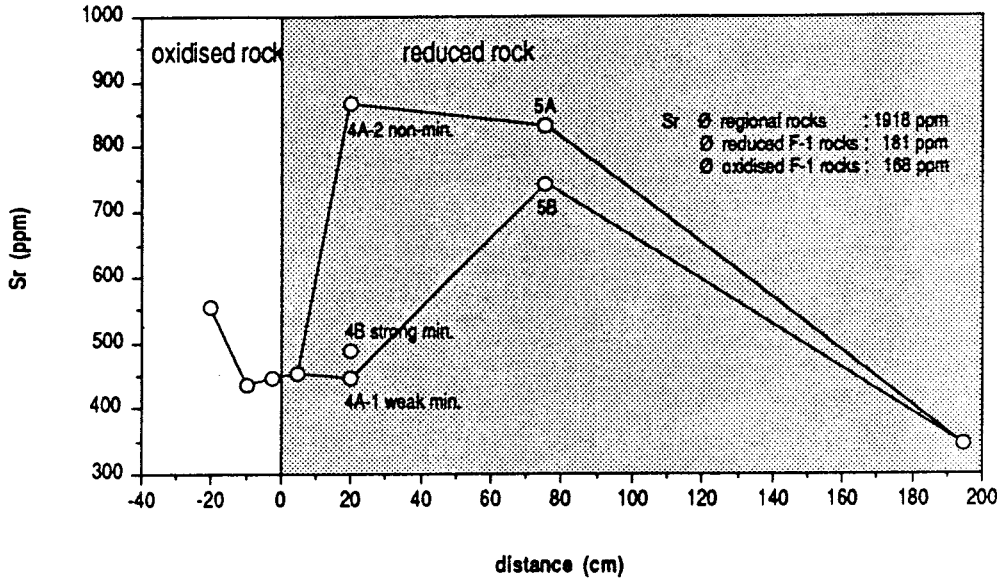

Figure 6-7. RFI redox front: geochemical distribution of Pb and Sr.

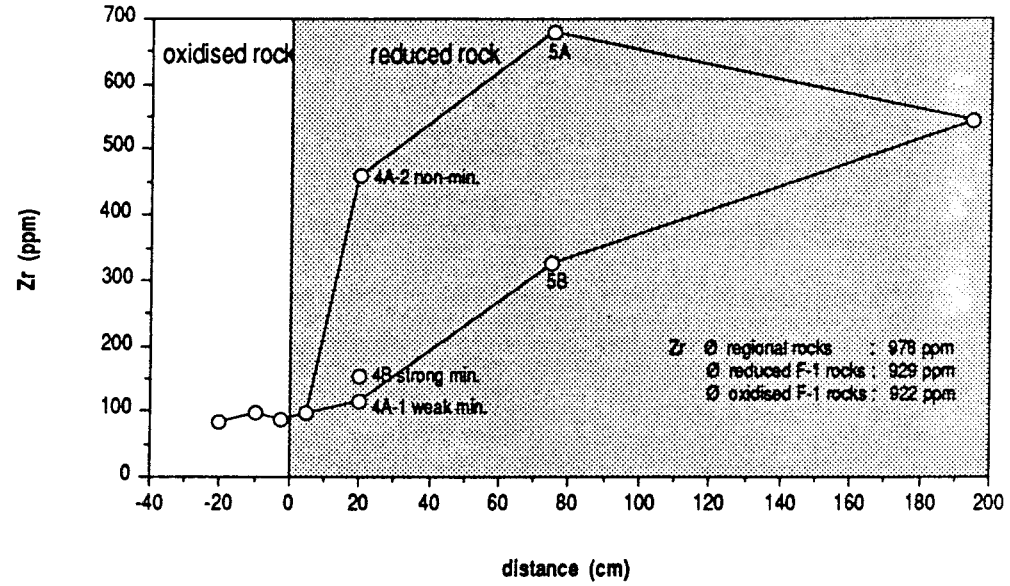

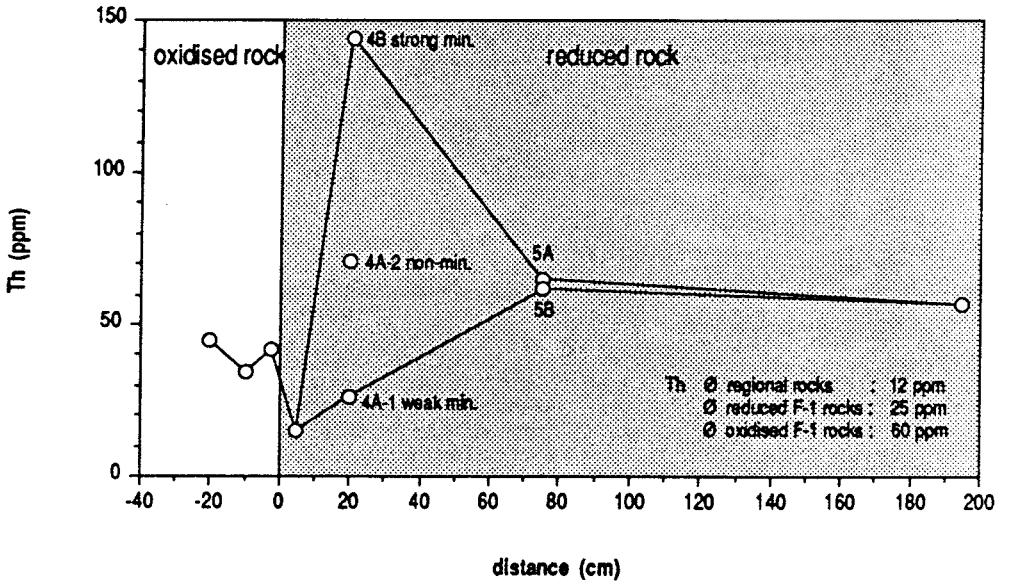

Figure 6-8. RFI redox front: geochemical distribution of Zr and Th.

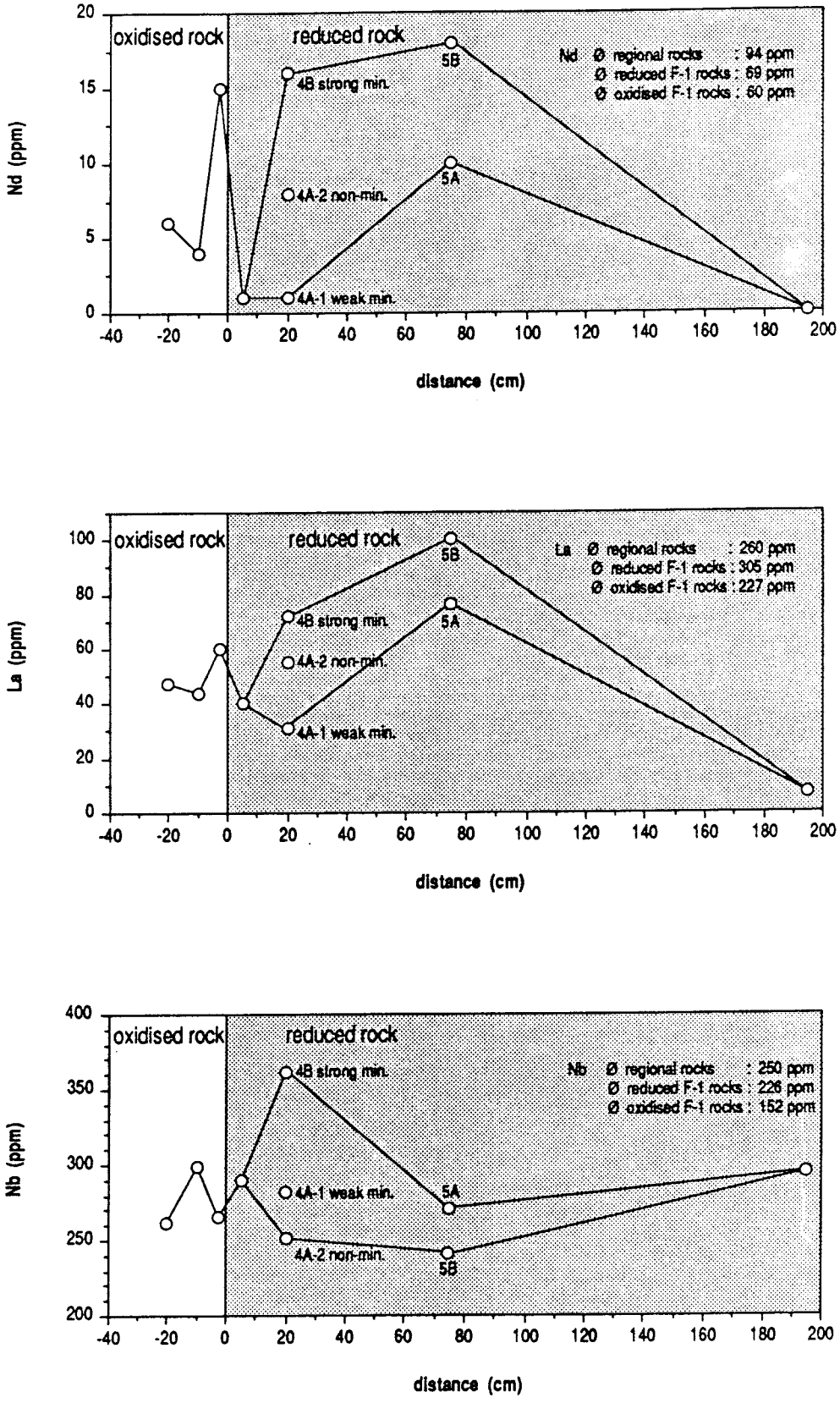

Figure 6-9. RFI redox front: geochemical distribution of Nd, La and Nb.

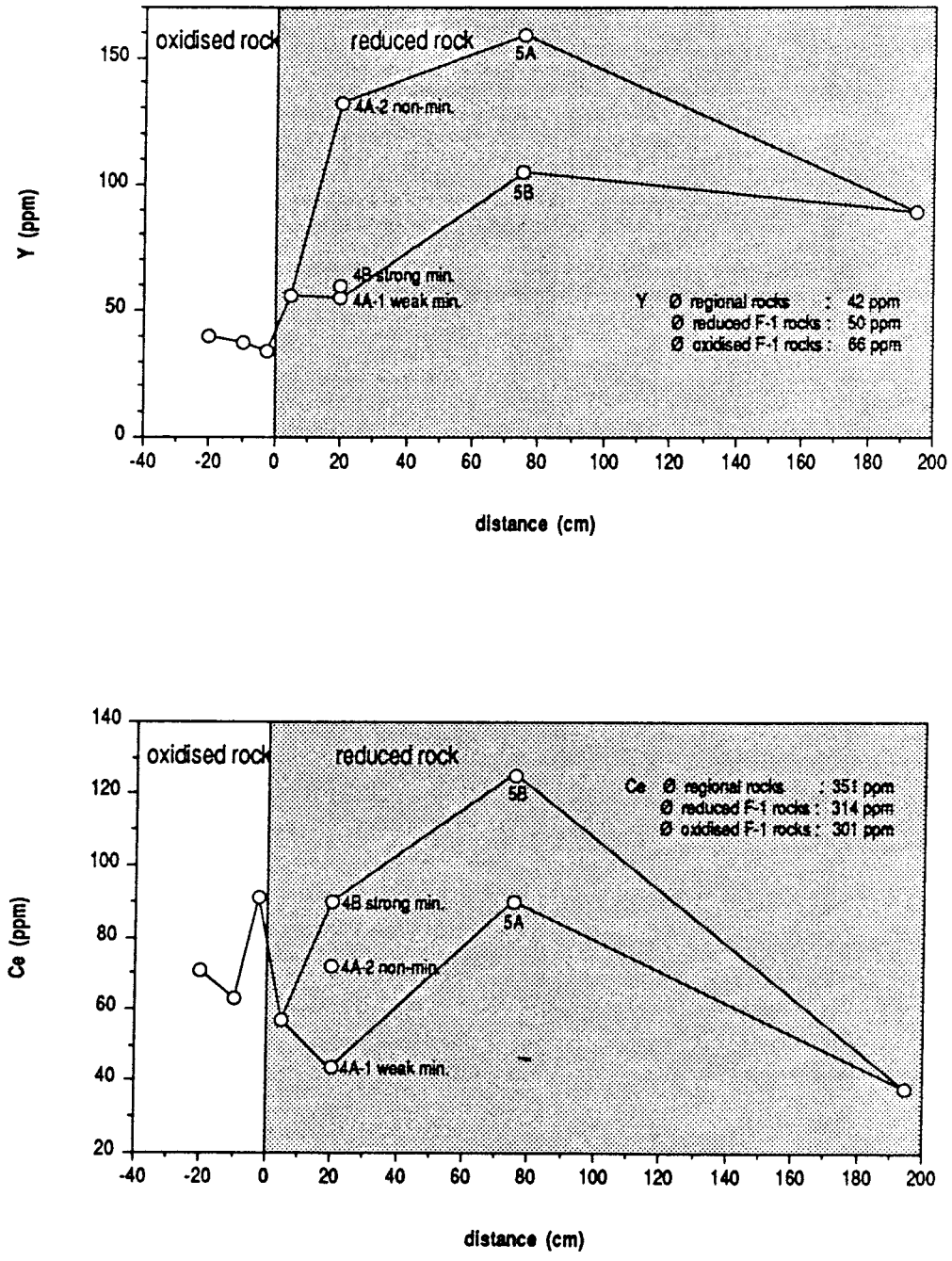

Figure 6-10. RFI redox front: geochemical distribution of Y and Ce.

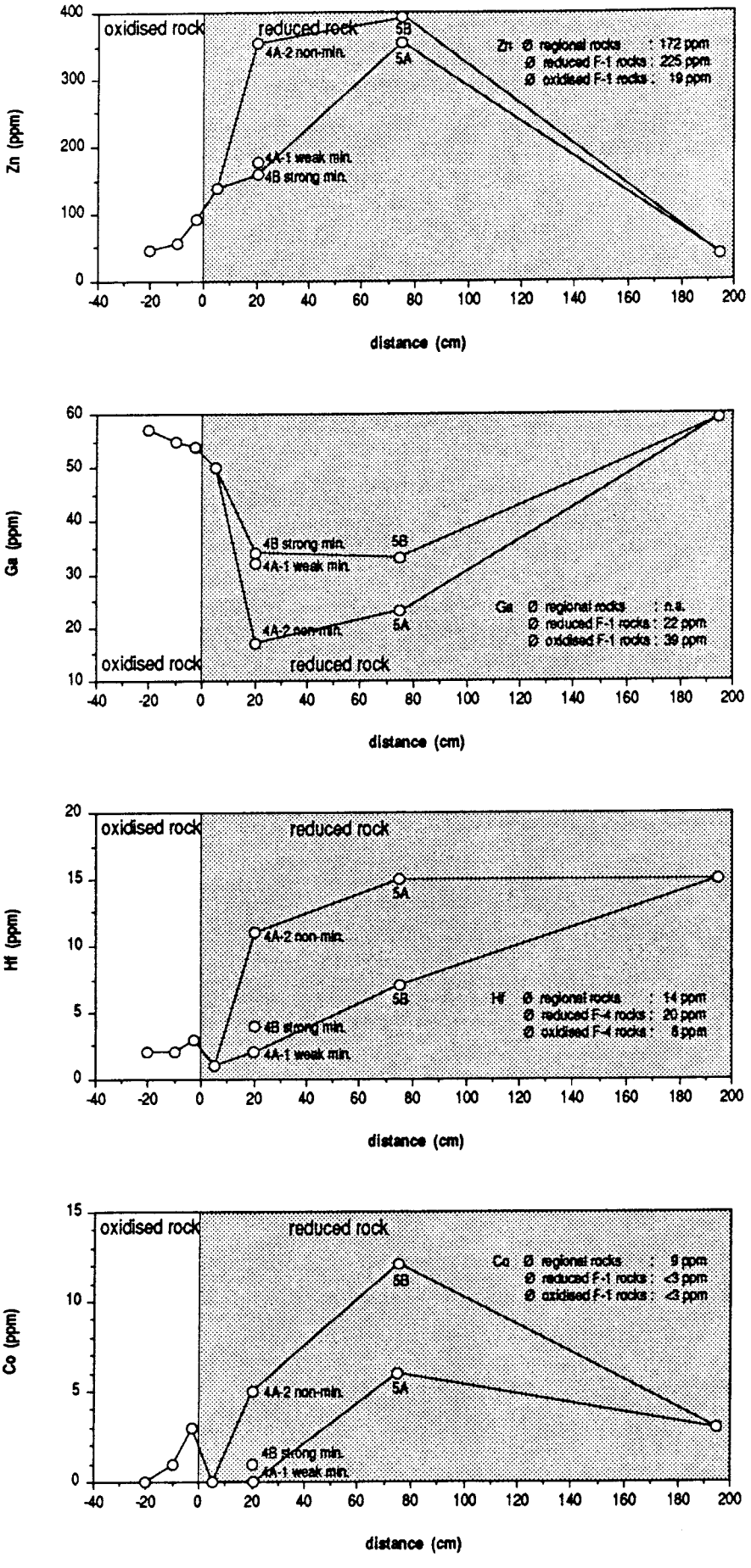

Figure 6-11. RFI redox front: geochemical distribution of Zn, Ga, Hf and Co.

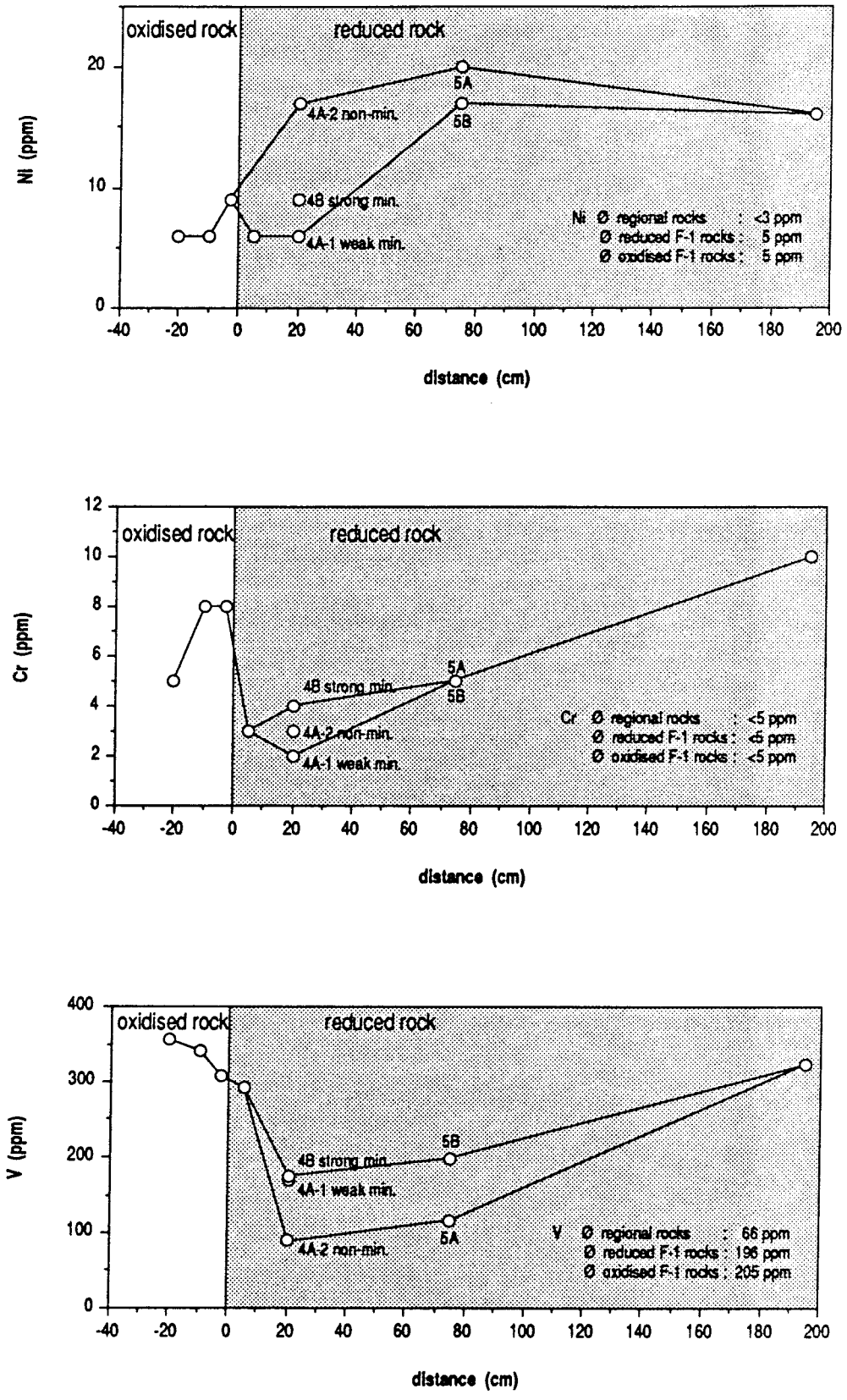

Figure 6-12. RFI redox front: geochemical distribution of Ni, Cr and V.

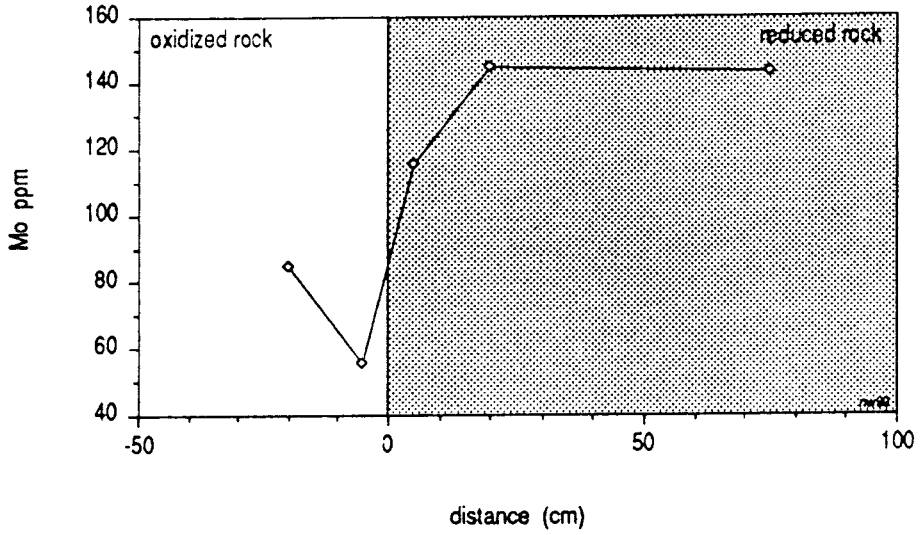

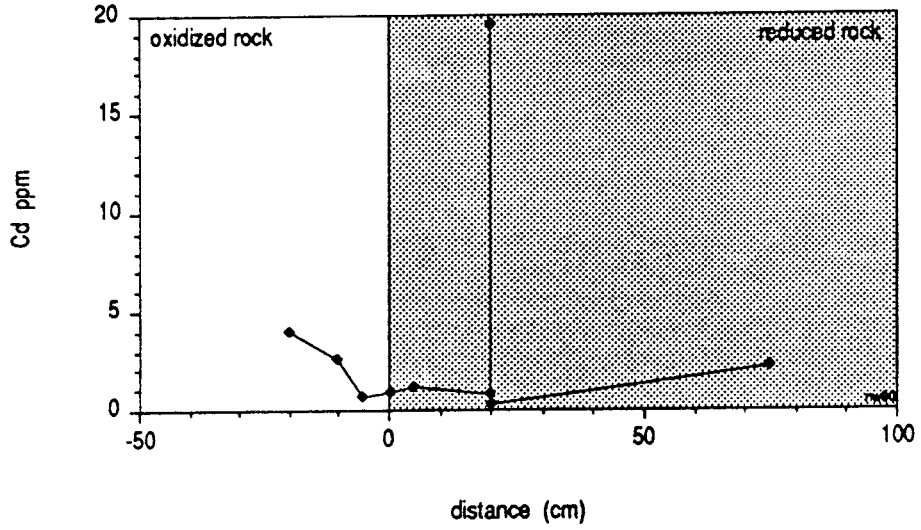

Figure 6-13. RFI redox front: geochemical distribution of Mo and Cd.

Hf, Zn, S and LOI are depleted; this is believed to be mainly due to redox front-related processes and not just the effect of natural rock compositional variations. However, sample RFI-3B is one of those included in the means of the RFI non-mineralised reduced rocks. The more mobile elements of the hydrothermal stage and of the redox front-related superimposed U-mineralisation were depleted, and the more immobile elements, including (?radiogenic) Pb, are enriched. The apparent mobility of Zr, Hf and, particularly, of Th and Y is surprising.

From the zone of maximum U-mineralisation, three subsamples representing different U-grades were analysed, including non-mineralised, weakly mineralised and strongly mineralised types (sample numbers RFI-4A-2; -4A-1 and -4B). They are considered together with samples RFI-5A and -5B of the non-mineralised and weakly mineralised reducing phonolites. It can be seen from the geochemical profiles that, of all the major and trace elements considered, only U precisely characterises the redox front-related U-mineralisation. Even Pb and Th are typically enriched in the highest grade U-mineralised rocks of RFI. In the low-grade (weak) U-mineralisations (samples RFI-4A-1 and -5B) both elements show insignificant variations, being either enriched or depleted in relation to the means of non-mineralised reducing rocks. Zr, Hf, Y and the analysed REEs show non-systematic variations with respect to the grade of the U-mineralisation related to the redox front, and most probably reflect just the rock compositional variations of magmatic and/or superimposed hydrothermal origin. However, this almost pure U-enrichment of the redox front mineralisation is characteristically very different from any of the hydrothermal (high-temperature) U-mineralisations. It characterises the redox front RFI, supported also by main and trace element geochemistry, as a low-temperature, geologically young (subrecent to recent) roll-front mineralisation.

The geochemistry of Cd

The presence of the CdS greenockite in massive pitchblende nodules from the Urânio do Brasil collections in Poços de Caldas has already been noted. Unfortunately these massive pitchblende nodules were only found during the early stages of mining at Osamu Utsumi, and details of their location are only qualitative. However, it is known that they were collected from the open pit in the oxidised rocks, at a few metres to a few tens of metres above the main redox front, overlying reduced rocks in areas of the higher grade U-mineralisations.

The nature and possible genetic relationships between these massive "fossil" nodules and those of the (subrecent to recent) active redox fronts observed in the mine (1st generation nodules) were judged to be of considerable interest to the project. As a result, the selective Cd mineralogy and geochemistry of the nodules were investigated.

Two series of analyses were carried out at the University of Bern. The first sample series included the main RFI oxidised and reduced bulk rock samples (Table 6-II; analyses 03; 04; 05; 06 and 07) and one sample consisting of the massive pitchblende zone of a large nodule (no. Ku-6, Waber *et al.*, this report; Appendix 1). This sample series confirmed the extremely high Cd content of the massive pitchblende nodule (approx. 0.1% Cd), although it was not selective enough to reveal any systematic variations of Cd along the RFI profile. Consequently a second, more selective sample set was prepared from the RFI samples by drilling minor sample portions of:

- oxidised bulk rock (with HFO minerals) adjacent to a bleached nodule resulting from pitchblende – pyrite dissolution;
- bleached nodules from pitchblende – pyrite dissolution (without HFO minerals) from oxidised rock;
- reduced bulk rock directly adjacent to, and about 5 cm from, the redox front (in the middle of the non-mineralised reduced zone);
- pitchblende macronodule from the zone of maximum U-mineralisation, and
- reduced bulk rock directly adjacent to the abovementioned macronodule, but without U-nodules and approx. 50 cm from the mineralised zone.

The results of the Cd analysis are shown in Table 6:2-IV (Appendix 6:2) and Figure 6-13. The figure shows the very good agreement of the two sample sets. Geochemically it is important to note that:

- bleached pitchblende nodules and enclosing typical oxidised rocks have identical Cd contents (pairs of analysis: 2-03 and 1-3);
- reduced non- or only weakly U-mineralised bulk rocks have low Cd contents, even if they are from the zone of maximum U-mineralisation and directly adjacent to pitchblende nodules;
- Cd is strongly and very selectively concentrated inside the pitchblende (macro-) nodules of RFI;

- directly adjacent to the redox front no specific Cd geochemical processes could be noted.

The enrichment/precipitation of Cd at the redox front is certainly related to the observed dissolution of sphalerite during the formation of the oxidised rocks. Its precipitation within the first generation pitchblende nodules, together with second generation pyrite and cryptocrystalline U-oxides, is very similar to the observations made in the case of the "fossil" massive pitchblende nodules. In the latter case, S-isotopes indicated a biochemical origin for the second generation pyrites (Waber *et al.*, this report; Appendix 1).

From the mineralogical-textural and geochemical evidence, it is believed that the related active redox front formation of (first generation) pitchblende nodules containing paragenetic second generation pyrite and Cd enrichments was facilitated by bio-geochemical processes, probably through the action of sulphate-reducing bacteria. Specific Cd minerals could not be identified. However, from analogy with the massive pitchblende nodules, it is believed that the Cd mineral in this case is also greenockite (CdS), present in such fine-grained and low total abundances that its detection using microscopic and XRD techniques is precluded.

According to the author, the observed precipitation of U-oxides, of Cd and related second generation pyrite exclusively within the microenvironments of the related redox front pitchblende nodules, and involving bacterial/bio-geochemical processes, is apparently an as yet unobserved geochemical association.

It is known from literature (Bambauer *et al.*, 1988, 1989) that Cd enters the oxidised Fe mineral jarosite under low-temperature weathering conditions. For the RFI sample (RFI-1C), which showed high U-contents and the possible presence of jarosite, unfortunately no Cd analyses exist. However, in the oxidised samples (RFI-1A, RFI-1B) the Cd-contents are higher than in the non-mineralised reduced rocks and it is positively correlated with the Fe_2O_{3tot} contents. In these cases this may indicate the coprecipitation of Cd with HFO minerals (mainly limonite).

7. Summary

Fundamental to all interpretations is the ability to distinguish the primary magmatic and later superimposed reducing hydrothermal processes from the final supergenic processes which resulted in bedrock oxidation and in the formation of the redox fronts.

The primary magmatic composition of the RFI rocks consisted of extremely fine-grained, almost aphanitic, weakly porphyritic (mainly orthoclase, nepheline and pseudoleucite phenocrysts) and (micro-)xenolithic (phonolite and nepheline syenite fragments) hololeucocratic volcanic phonolites. Geochemically they are silica-unsaturated peralkaline rocks, particularly rich in K_2O and Zr, La, Ce and Nd when compared to the regional magmatic rocks. Primary magmatic differences between the RFI phonolite samples could not be detected.

Post-magmatic, pneumatolytic and auto-hydrothermal processes (earlier than the potassic rock hydrothermal alteration) could not be identified. If present, such processes are normally quite weak in rapidly cooled volcanic rocks.

The potassic rock reducing hydrothermal alteration, associated with weak (hydrothermal) U- (Th) – Zr (Hf) – Y mineralisation, is responsible for the main present-day characteristics of the RFI rocks. Globally, one can consider the governing mineralogical processes as K-feldspathisation (through exchange reactions), sericitisation/illitisation associated with argillation (major kaolinisation and minor smectite formation) and pyritisation. Chemically, the main processes involved alkali exchange reactions resulting in K enrichment, SiO_2, Al_2O_3 and Rb enrichments and Sr losses. Physical parameters such as porosity increased, together with a lower global density and higher grain (solids) density. The penecontemporaneous but irregular mineralisation (of U, Th, Zr, Hf, Y and others) is considered to be the main factor explaining the localised heterogeneous geochemical (and mineralogical) trace element (and minor mineral) variations observed between the non- or weakly redox front-affected RFI rocks.

The redox front processes, in fact, appear to have had only a very restricted mineralogical and geochemical influence. In the reduced rocks these processes resulted in a zone of more important U-mineralisation with certain analogies to the 'roll-front type' that consists of nodular pitchblende. The U-nodules contain 2 pyrite generations, an unidentified Cd mineral (probably CdS-greenockite) and the rock-forming minerals. Most probably they formed in association with bio-geochemical activity involving sulphate-reducing bacteria. Such microbial activity is discussed in more detail in West *et al.* (this report series; Rep. 10). Geochemically the related redox front U-mineralisations are mainly characterised by the U-enrichment itself, minor Th and (?radiogenic) Pb enrichment, and very selective Cd enrichment (only in the U nodules).

The oxidic redox front-related processes are restricted to a very proximal zone; in the case of RFI within a zone of less than 5 cm directly adjacent to the redox front. Geochemical processes consist essentially of an (oxidic) enrichment of Fe, U and

(sulphate) S. Mineralogically, the formation of HFO minerals (mainly limonite) could be observed and the formation of Fe(III)-sulphates (possibly of the jarosite type) inferred. The oxidised Fe species are considered the most important phases for explaining the other systematic trace element variations observed in the direct vicinity of the redox front.

A few more centimetres distant, the influence of the redox front disappears and the 'normal' oxidised rocks show only minor mineralogical and geochemical alterations typical of incipient lateritic weathering, i.e. the formation of a second kaolinite generation correlated with Al and Ga enrichment and U-loss.

8. References

Bambauer, H.U., Gebhard, G., Holzapfel, Th. and Krause, Chr., 1988. Schadstoff-Immobilisierung in Stabilisaten aus Braunkohlenaschen und REA-Produkten. *Fortschr. Miner.*, 66, 2, 281-290.

Bambauer, H.U., Steffes-Tun, W. and Krause, Chr., 1989. Immobilization of thallium in a pyrite ash dump by jarosite formation. Inter. Conf. on Applied Mineralogy (GAC-MAC-ICAM-CAM), *GAC-MAC Ann. Meet.*, Program with Abstracts, Vol. 14, p. A 118, Montreal.

Barrington, J. and Kerr, P.F., 1961. Uranium mineralisation at the Midnite Mine, Spokane, Washington. *Econ. Geol.*, 56, 241-258.

Blanchard, R., 1968. Interpretation of leached outcrops. *Nevada Bureau of Mines, Bull.*, 66 (chapt. 7), Nevada Bureau of Mines & Geology, Univ. of Nevada, Reno, Nevada, 196 pp.

Goldschmidt, V.M., 1954. Geochemistry. *Clarendon Press*, Oxford, 730 pp.

Le Maître, R.W., 1984. A proposal by USGS-Subcommission on the systematics of igneous rocks for a chemical classification of volcanic rocks based on the total alkali silica (TAS) diagram. *Austral. J. Earth Sci.*, 31, 243-255.

O'Neil, J.R. and Taylor, H.P. Jr., 1967. The oxygen isotope and cation exchange chemistry of feldspars. *Amer. Miner.*, 52, 1414-1437.

Porto da Silveira, C.L., 1986. Geoquímica da mineralização metassomática urano-sódica de Espinharas (PB). *PhD-thesis* (unpubl.), Dept. of Chemistry, PUC-RJ (Pontifícia Universidade Católica do Rio de Janeiro), 287 pp.

Porto da Silveira, C.L., Schorscher, H.D. and Miekeley, N., 1989. The geochemistry of albitization and related U-mineralization, Espinharas, Pb, Brazil. *13th Inter. Geochem. Explor. Symp.*, Abstracts, 101-102, co-publ. SBGq-CPRM/DNPM, Rio de Janeiro.

Ramdohr, P., 1975. Die Erzmineralien und ihre Verwachsungen. 4th ed., *Akademie-Verlag*, Berlin, 1277 pp.

Rogers, J.J.W. and Adams, J.A.S., 1978. Thorium (part E). In: K.H Wedepohl (Editor), Handbook of Geochemistry, Vol. II-5, *Springer*, Berlin, Heidelberg, New York.

Swanson, H.E. and Fuyat, R.K., 1953. Standard X-ray diffraction powder patterns, V.II: *NBS Circular 539*, p. 33 (cit. in: Barrington and Kerr, 1961).

Ulbrich, M.N.C., 1983. Aspectos mineralógicos e petrológicos de nefelina sienitos do maciço alcalino de Poços de Caldas, MG-SP, *PhD-thesis* (unpubl.), University of São Paulo, 369 pp.

Ulbrich, M.N.C., Gomes, C.B. de and Ulbrich, H.H.G.J., 1984. Nefelina sienitos do maciço alcalino de Poços de Caldas MG-SP: caracterização mineralógica e petrológica. *33° Cong. Bras. Geol.*, anais, 4.362–4.376 (Vol. IX), Rio de Janeiro.

Appendix 6:1

PLATES 6:1-1 – 6:1-9.

PLATE 6:1-1. Composed sample RFI-2 of oxidised phonolite, yellow-brown in colour (lower major portion of the sample), separated from the reduced phonolite of white-grey colour (uppermost part of the sample) by the sharp redox front. The white nodules in the oxidised rock resulted from the dissolution of former pitchblende nodules by the progressive redox front. Note nodule alignment (in partial preservation) along the lowermost part of the sample delimiting a cleaved fracture face.

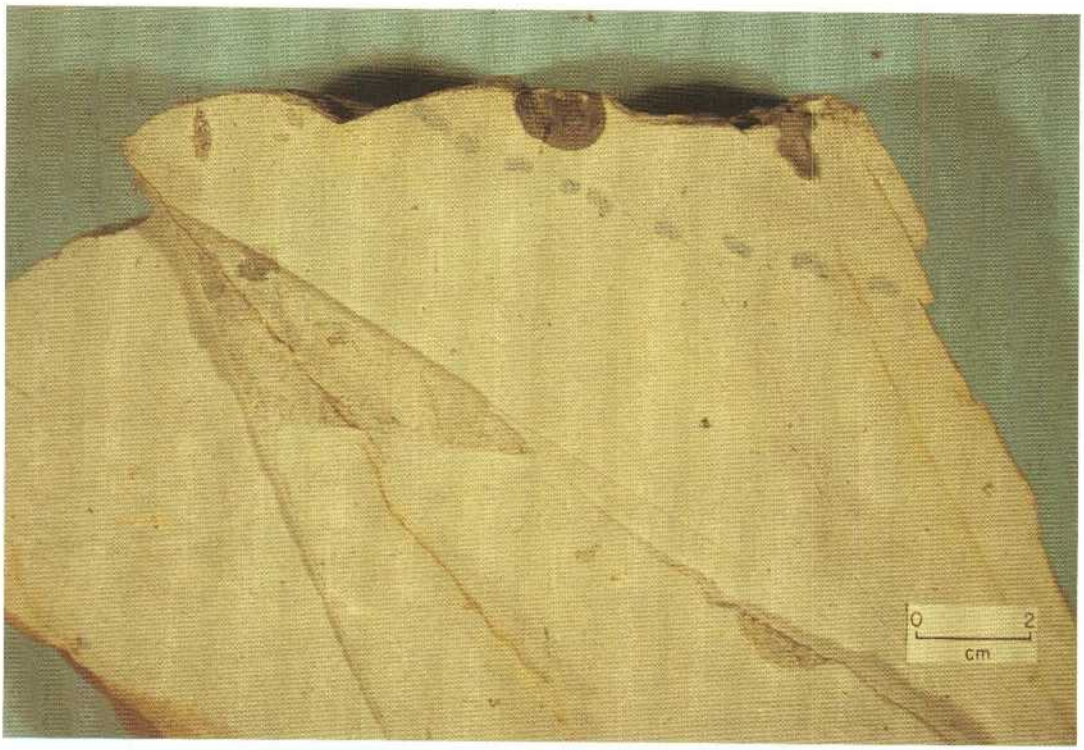

PLATE 6:1-2. Detail of the redox front and oxidised phonolite from sample RFI-2 (PLATE 6:1-1). Note "oscillatory zoning" of HFO (hydrous ferric oxides – mainly limonite) distributions, and that the oxidation may be incomplete even in residual zones of the oxidised phonolite clearly left behind by the passage of the redox front (e.g. in the right-hand lower portion of the sample that shows greyish colours unaffected by brown HFO staining). Note also that the dissolution of the pyrite-enriched pitchblende nodules occurred without the precipitation of "indigenous" HFO, thus resulting in white, particularly HFO-poor nodules/rock portions.

PLATE 6:1-3. Composed sample RFI-3 comprising minor portions of oxidised phonolite and redox front (in the extreme lowermost left-hand part of the sample), reduced phonolite of whitish-grey colouration without pitchblende nodules, forming an approximately 10 cm wide zone directly preceding the redox front (major, central part of the sample) and reduced phonolite with pitchblende nodules (black) of zone of maximum (redox front-related) U-mineralisation (right-hand topmost part of the sample, delimitated approximately by the dashed markings). Note the fine-grained (micro-)xenolithic nature of the phonolite and the fracture related/controlled formation of the pitchblende nodules. At the top edge of the sample a delimiting (horizontal) fracture controls both visible nodules. However, in addition, the right-hand nodule shows more clearly the influence of a second fracture system that intersects the horizontal fracture system obliquely at a steep angle (running parallel to the right-hand delimitation of the sample).

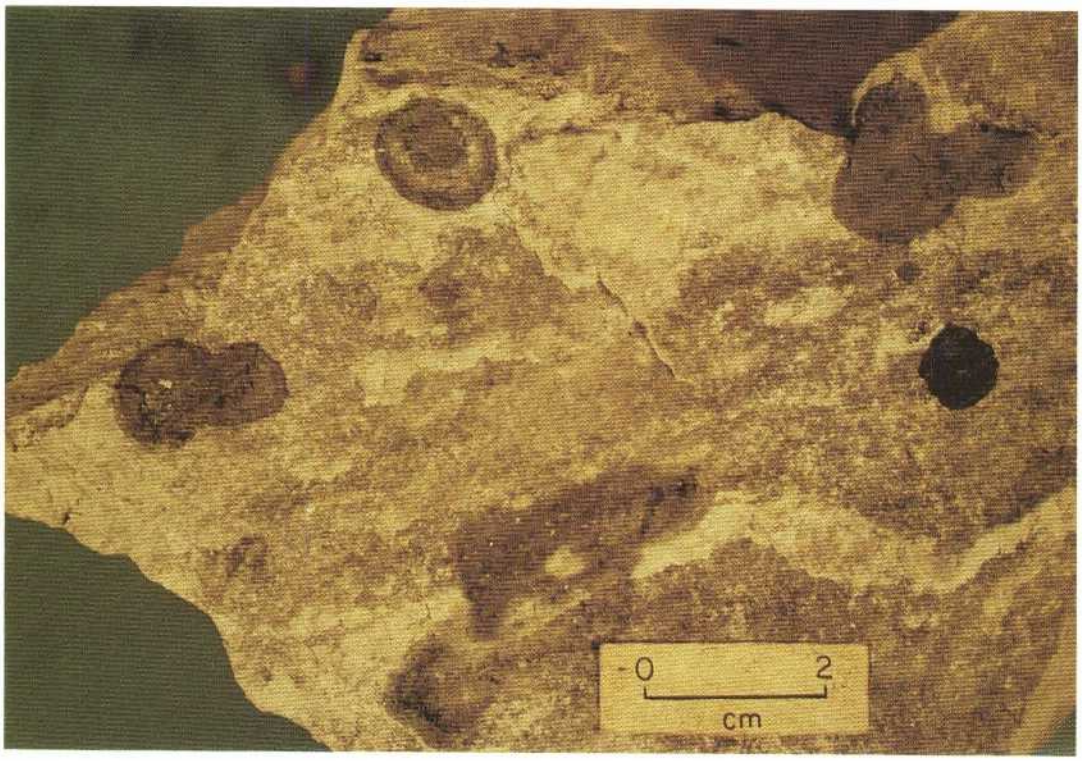

PLATE 6:1-4. Sample RFI-4 of reduced phonolite from the zone of maximum (redox front- related) U-mineralisation. The view is from a highly mineralised natural fracture plane containing five major pitchblende nodules that crosscut the mineralised zone in the reduced phonolite. Note the different densities of the pitchblende impregnation in the nodules (shown by the colour variations from totally black decreasing to medium grey), the forms of the circular, irregular and composed nodules, and the internal textures of homogeneous nodules (right-hand middle and top of sample) and inhomogeneous nodules. The latter show regular concentric zoning (left-hand middle and top of the sample) or irregular zoning (composed nodule touched by the upper left-hand corner of the scale). It should, however, be noted that the 3-dimensional forms of the nodules are normally flat-lenticular and only very rarely thick-lenticular to subspherical. Maximum cross sections always occur on the faces of the fracture planes.

PLATE 6:1-5. Reduced phonolite (sample RFI-5) about 35 cm away from the zone of maximum U-mineralisation (cf. Fig. 6-1). Note the very fine-grained rock groundmass, the content of microxenoliths, and the microporosities.

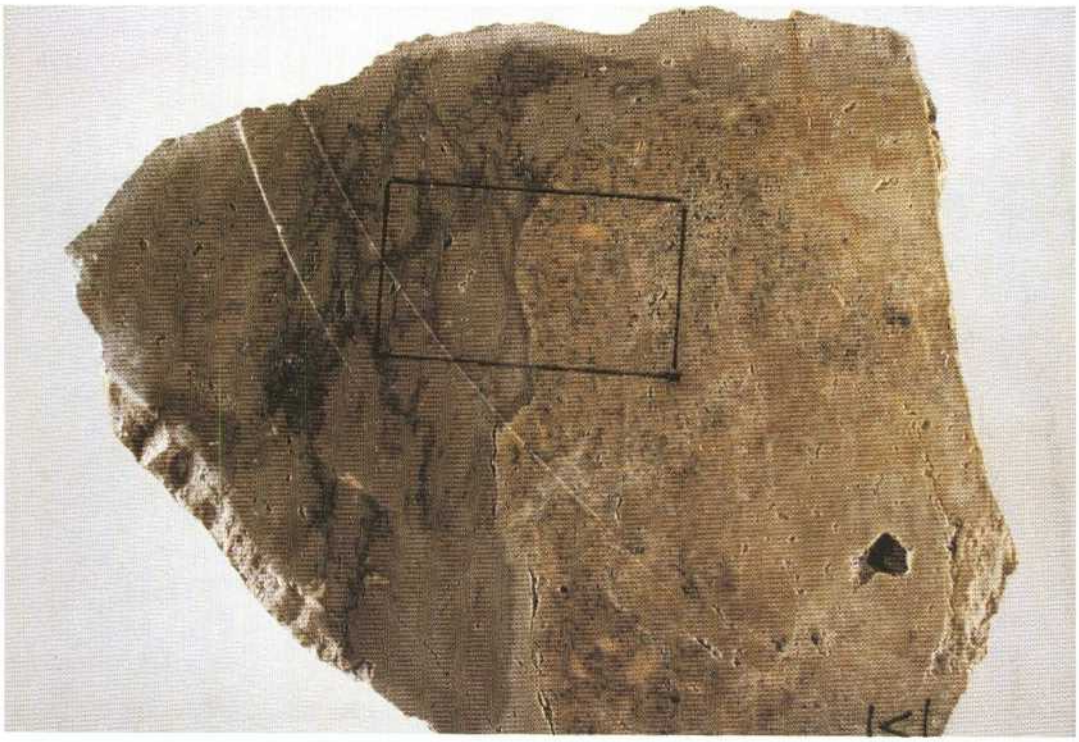

PLATE 6:1-6. Reduced composite rock sample (RFI-6) collected about 1 m away from sample RFI-5 (cf. Fig. 6-1). The sample comprises a larger sized reduced nepheline syenite xenolith (right-hand side) of medium to coarse grain-size and lighter colours, enclosed by a very fine-grained reduced phonolite (left-hand side). The phonolite shows medium grey colours with dark grey veining (due to absorbed moisture during preparation) and a microporosity and flow orientation subparallel to the contact with the nepheline syenite xenolith. The phonolite and nepheline syenite portions were separately prepared and studied (about 4/5 of nat. size; see rectangular thin section mark across phonolite/nepheline syenite contact).

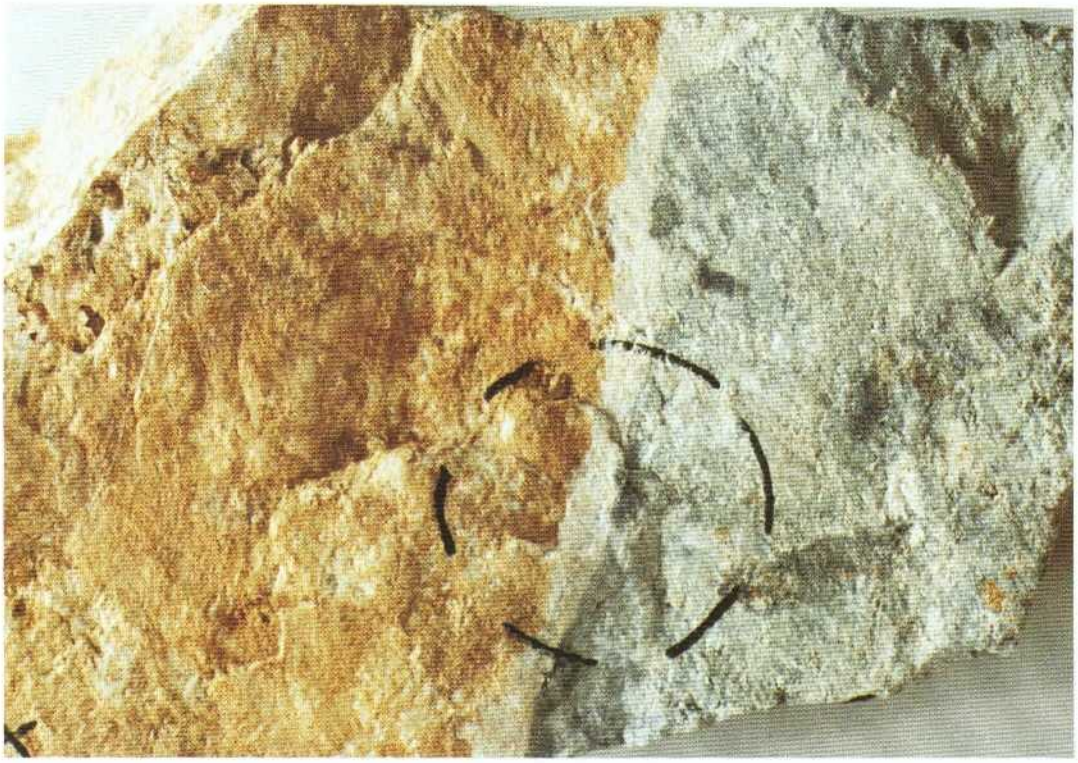

PLATE 6:1-7. Redox front in a fine-grained phonolite (sample U – 7G; near open pit coordinates: 8.1 KK; about 1.6 x nat. size), showing the development of a narrow zone (of millimetric width) free from U-mineralisation, but pyrite-bearing (white coloured), crossing the centre of the hand specimen. The zone separates the reduced and U-mineralised portion of the sample (medium grey colouration and containing dark grey rounded irregular shaped, not very well defined pitchblende nodules of low U-oxide grade; right-hand side of the photograph) from the oxidised part (yellow-brown colouration after hydrolysis and HFO mineral (mainly limonite)-precipitation; left-hand side). The white zone is not a kaolinite/clay mineral layer, but simply a reduced and bleached rock zone identical in composition with the adjacent areas which are characterised by total U-oxide dissolution associated, probably, with incipient sulphide mineral (including pyrite)-dissolution. Note the sharp dissolution boundary of dark grey pitchblende nodules towards the white zone.

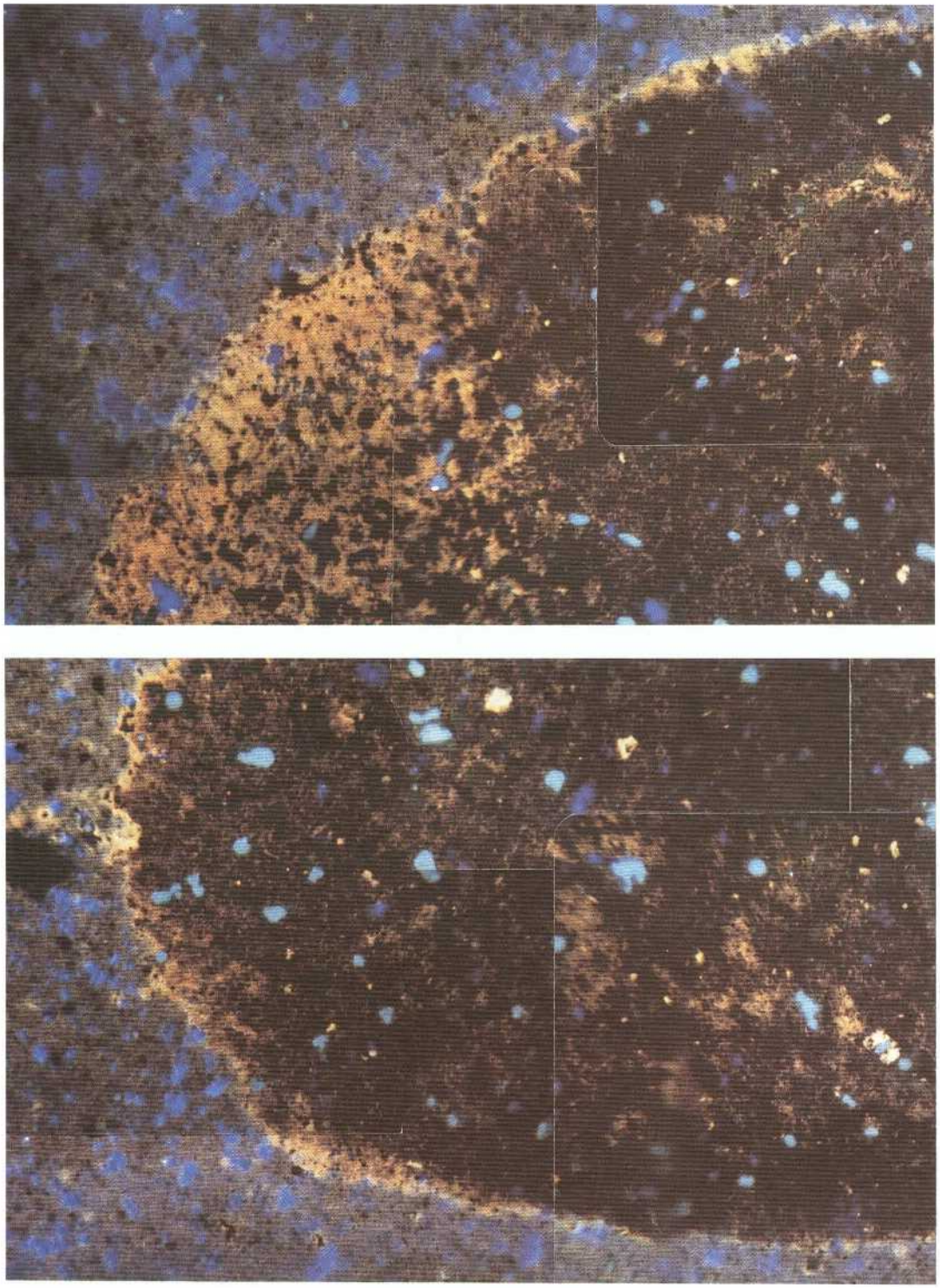

PLATE 6:1-8. Cathodoluminescence image of (two quarters of) a pitchblende nodule of total maximum diameter about 10 mm from a redox front in fine-grained phonolite. Note the non-emission of pitchblende impregnated (dark to black) portions of the nodule and the light yellowish-reddish emission of the illite – K-feldspar – kaolinite silicate mineral matrix of the nodule after pitchblende dissolution along the borders and in the left-hand part of the nodule (seen only in the upper photograph). Open pores in the nodule show light-blue or dark-(ink) blue emission (depending on the presence of preparation adhesives covering the glass support of the polished rock thin section) and dark- (ink) blue emission, if within the surrounding silicate matrix of the nodule (which was better impregnated by the preparation adhesives). The emission colours of the surrounding rock matrix are medium yellowish-grey and the finely disseminated black minerals are non-emitting (mostly submillimetric) pyrites. Compare with same nodule in plain light view (PLATE 6:1-9).

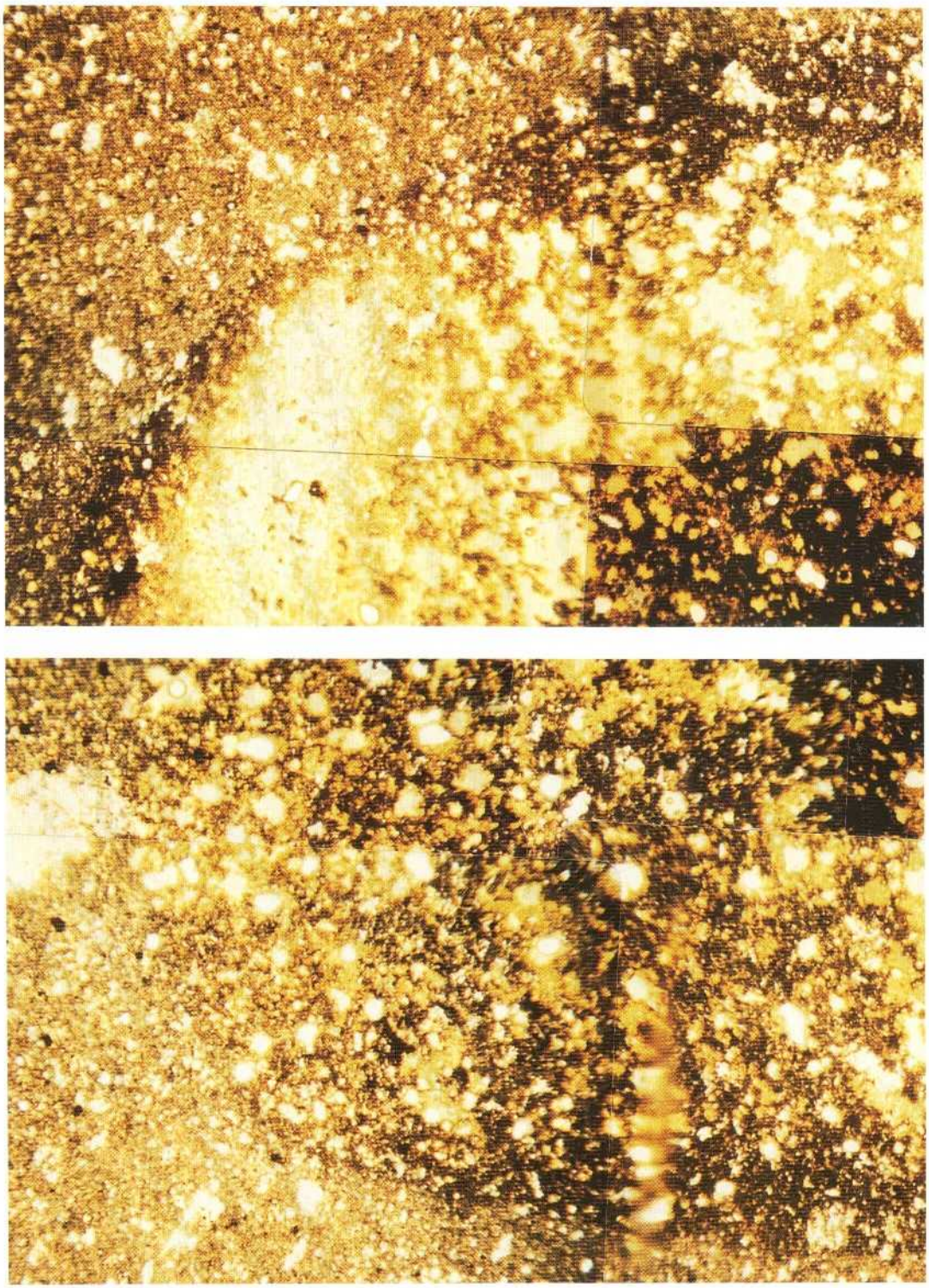

PLATE 6:1-9. Plain light, equal magnification view of the same pitchblende nodule shown in PLATE 6:1-8. Note the variable density distribution and the type of pitchblende impregnation within the nodule (black-opaque with maximum density and very dark brown-semitranslucent with less dense cryptocrystalline pigmentations). The leached uranium barren parts of the nodule are the bright, light yellow translucent portions. The surrounding rock mass is fine-grained and contains abundant opaque (black coloured) pyrite microcrystals.

Appendix 6:2

Rock chemical data for RFI.

Appendix 6:2
Rock chemical data for RFI.

TABLE 6:2-I

Chemical data for sample set I (Table 6-II) comprising large-sized samples.

Sample no. (Anal. no.)	Analytical methods and elements: Classic (wt.%) S[1]	Fe_2O_3tot[1]	FeO[1]	LOI[1]	AAS (ppm) Mo[1]	Cd[2]	Petrography
RFI-1A (03)	0.13	1.63	<0.2	2.87	85	4.0	Oxidised rock 25-15 cm from redox front
RFI-2B (04)	0.09	1.10	<0.2	1.88	55	0.658	Oxidised rock 10-0 cm from redox front
RFI-3B (05)	0.55	0.48	<0.2	2.29	115	1.1	Reduced rock 0-10 cm from redox front; pyrite-bearing
RFI-4B (06)	0.55	0.46	<0.2	2.01	145	0.788	Reduced rock of max. U-mineralisation; pyrite-bearing
RFI-5B (07)	1.09	1.05	<0.2	3.38	143	2.2	Reduced rock ~70-90 cm from redox front; pyrite-bearing

Analysis carried out by:

[1]Paulo Abib Engenharia S.A., São Paulo;
[2]University of Bern.

LOI was determined at 900°C.

FeO analysis was not successful (as shown by the results indicating below detection limit values obtained for the reduced pyrite-bearing rocks, probably due to the presence of greater amounts of oxidised uranium).

Cd values represent the results from triplicate analysis.

TABLE 6:2-II
XRF analysis of sample set II (Table 6-II) selected from detailed sampling of RFI.

Elements (wt.%)	RFI-1A ox. Ph.	RFI-1B ox. Ph.	RFI-1C ox. Ph.	RFI-3 red. Ph.	RFI-4A-1 red. Ph.	RFI-4A-2 red. Ph.	RFI-4B red. Ph.	RFI-5A red. Ph.	RFI-5B red. Ph.	RFI-6B red. NeS-x
SiO_2	59.9	59.42	58.45	60.06	60.9	60.83	60	60.42	59.31	58.45
TiO_2	0.46	0.53	0.46	0.49	0.45	0.41	0.43	0.41	0.42	0.57
Al_2O_3	22.41	22.05	22.07	22.11	20.93	20.04	21.42	20.48	21.05	23.39
Fe_2O_3	1.37	2.06	2.52	0.97	1	0.93	0.9	1.35	1.74	1.24
MnO	0.01	0.01	0.01	0.01	0.01	0.01	0.01	0.01	0.01	0.01
MgO	0.14	0.1	0.1	0.1	0.1	0.1	0.1	0.1	0.1	0.1
CaO	0.03	0.01	0.01	0.01	0.01	0.01	0.01	0.01	0.01	0.01
Na_2O	0.01	0.01	0.01	0.01	0.01	0.01	0.01	0.01	0.01	0.01
K_2O	14.23	14.18	14.04	14.36	14.48	14.51	14.06	14.11	13.87	13.26
P_2O_3	0.1	0.09	0.09	0.09	0.08	0.14	0.09	0.14	0.13	0.07
H_2O	2.29	2.35	2.8	2.32	2.35	2.82	2.65	3.35	3.68	3.5
Total wt.%	100.95	100.81	100.56	100.53	100.32	99.81	99.68	100.39	100.33	100.61
Ba (ppm)	327	285	235	225	198	483	114	292	293	523
Rb	284	283	287	282	273	253	320	258	254	273
Sr	554	436	448	454	445	869	488	834	743	345
Pb	16	22	30	91	78	37	195	32	31	27
Th	45	34	42	15	26	71	144	65	62	57
U	106	130	861	175	448	121	4876	204	660	84
Nb	262	299	266	290	282	251	361	270	241	295
La	47	44	60	40	31	55	72	76	100	7
Ce	71	63	91	57	44	72	90	90	125	38
Nd	6	4	15	1	1	8	16	10	18	0
Y	40	37	34	56	55	132	59	159	105	89
Zr	82	97	86	99	114	459	153	678	326	545
V	357	342	307	293	170	91	175	115	197	322
Cr	5	8	8	3	2	3	4	5	5	10
Ni	6	6	9	6	6	17	9	20	17	16
Co	0	1	3	0	0	5	1	6	12	3
Cu	0	0	0	0	0	0	0	0	0	0
Zn	46	56	93	139	177	353	158	354	392	38
Ga	57	55	54	50	32	17	34	23	33	59
Hf	2	2	3	1	2	11	4	15	7	15
S	1039	1534	27354	4536	9196	12956	10359	13162	15532	58618

Analysis carried out by the University of Bern.

red. Ph. – reduced phonolite
ox. Ph. – oxidised phonolite
red. NeS-x – reduced nepheline syenite xenolith

TABLE 6:2-III

Mean compositions from oxidised and reduced, non-mineralised and mineralised RFI and F1 rocks, and from the regional magmatic nepheline syenites and phonolites.

Oxides	Redox front-1 rocks				Borehole F1 rocks		Regional rocks (10)
	Oxidised (3)		Reduced (7)		Oxidised (16)	Reduced (29)	
(wt.%)	U<210 ppm(2)	U = 861 ppm(1)	U<210 ppm(4)	U>210 ppm(3)	U<310 ppm	U<210 ppm	U<5 ppm
SiO_2	59.66	58.45	59.94	60.07	56.00	56.17	52.86
TiO_2	0.50	0.46	0.47	0.43	0.47	0.45	0.64
Al_2O_3	22.23	22.07	21.51	21.13	23.37	21.77	19.53
Fe_2O_{3tot}	1.72	2.52	1.12	1.21	2.92	3.05	3.96
MnO	0.01	0.01	0.01	0.01	<0.01	0.08	0.24
MgO	0.12	0.10	0.10	0.10	0.05	0.07	0.28
CaO	0.02	0.01	0.01	0.01	0.01	0.14	1.70
Na_2O	0.01	0.01	0.01	0.01	0.68	0.38	7.49
K_2O	14.21	14.04	14.06	14.14	13.02	13.40	8.16
P_2O_5	0.10	0.09	0.11	0.10	0.05	0.05	0.08
LOI	2.32	2.80	3.00	2.89	3.11	3.54	1.75
Total wt.%	100.88	100.56	100.34	100.11	99.68	99.10	96.68
Ba (ppm)	306	236	381[1)]334[2)]	202	972	614	252[1)]50[2)]
Rb	284	287	267	282	338	298	154
Sr	495	448	626	559	168	181	1.913
Pb	19	30	47	101	25	<6	6
Th	40	42	52	77	60	25	9
U	118	861	146	1.995	89	32	<5
Nb	281	266	277	295	152	226	249
La	46	60	45	68	227	305	263
Ce	67	91	64	86	301	314	350
Nd	5	15	5	12	60	69	92
Y	39	34	109	73	66	50	41
Zr	90	86	445	198	922	929	965
V	350	307	205	181	205	196	67
Cr	7	8	<6	<6	<6	<6	<6
Ni	6	9	15	11	5	5	<3
Co	<8	<8	<8	<8	<8	<8	9
Cu	<3	<3	<3	<3	4	<3	<3
Zn	51	93	121	242	19	225	168
Ga	56	54	37	33	39	22	n.a.
Hf	2	3	11	4	n.a.	n.a.	12
Sc	n.a.	n.a.	n.a.	n.a.	4	2	<1
F	n.a.	n.a.	n.a.	n.a.	1.158	1.638	1.757
S	1.287	27.354	22.318	11.696	<50	8.790	928

TABLE 6:2-III (contd.).

Borehole F1 oxidised means include samples:

1-1B; 10-1A; 14-1A; 16-1A; 20-1B; 26-1A; 31-1A; 33-1A; 34-1B; 43-1A; 1-1C; 20-1A; 23-1A; 47-1A; 55-1A; 59-1B.

Excluding sample 1-1C the following trace element means were determined:

Zr = 7.847 ppm; V = 1.352 ppm; Y = 206 ppm;

20-1A: Ce = 1.606 ppm;

23-1A: La = 1.498 ppm; Ce = 1.276 ppm; Nd = 288 ppm;

47-1A: Ce = 2.331 ppm.

Borehole F1 reduced means include samples:

39-1A; 74-1A; 75-1B; 77-1A; 81-1A; 85-1A; 90-1B; 101-1A; 106-1A; 111-1A; 112-1A; 119-1A; 121-1A; 126-1A; 68-1A top; 68-1A mid; 68-1A bot; 69-1B; 71-1A; 75-1B; 77-1B; 78-1A; 109-1B; 112-1AD; 113-1B; 117-1A; 126-1A; 126-1B.

Excluding 74-1A the following trace element means were determined:

La = 6.843 ppm; Ce = 6.272 ppm; Nd = 1.854 ppm; Y = 461 ppm.

1) = means of all the rocks;

2) = number of analysed phonolites;

n.a. = not analysed;

(n) = number of analysed rocks.

TABLE 6:2-IV

Cadmium AAS analysis from RFI samples.

Sample no.	Analysis no.	Cd	Petrography of analysed sample fraction
RFI-1A	03	4.0 ppm	Oxidised bulk phonolite; ~25–15 cm from the redox front
RFI-2B	04	658 ppb	Oxidised bulk phonolite; ~10 cm adjacent to the redox front
RFI-3B	05	1.1 ppm	Reduced bulk phonolite, non-mineralised zone ~10 cm wide, adjacent to the redox front
RFI-4B	06	788 ppb	Reduced bulk phonolite (without pitchblende nodules) from zone of max. U-mineralisation
RFI-5B	07	2.2 ppm	Reduced bulk phonolite weakly U-mineralised (with pitchblende micronodules)
RFI-1B/2A	1	4.1 ppm	Bleached nodules from samples RFI-1/2 (mixed sample)
RFI-1A	2	2.6 ppm	Bleached nodule from sample RFI-1A
RFI-1B/2A	3	3.0 ppm	Oxidised bulk phonolite (mixed material adjacent to bleached nodules; sample RFI-1/2)
RFI-2C	4	844 ppb	Reduced bulk phonolite; ~0.5 cm from the redox front
RFI-3B	5	1.0 ppm	Reduced bulk phonolite; ~5 cm from the redox front (middle of non-mineralised zone)
RFI-4B	6	19.5 ppm	Pitchblende nodule from sample RFI-4B
RFI-4B	7	307 ppb	Reduced bulk phonolite directly adjacent to pitchblende nodule RFI-4B
KU-6	KU-6	≥1.000 ppm	Massive pitchblende nodule ("fossil" nodule) containing microscopic CdS greenockite; from the Urânio do Brasil collection (semiquantitative analysis)